Chapter 7

Study of effect of α-Synuclein mutants on its interaction with the lipid membrane

Study of effect of α-Synuclein mutants on its interaction with the lipid membrane

7.1. Abstract:

Based on genetic investigation, point mutations such as A30P, A53E, A53T, E46K, G51D and H50Q in the N-terminal region, have been linked to family forms of PD. The influence of the various α-Syn variations on the parameters of membrane binding and aggregation formation varies. Accordingly, the conformational investigation of α-Syn mutants and its subsequent effect on the membrane-protein interaction has been studied using all-atom MD simulation. The overall membrane order parameters were determined to ensure the stabilization of the multicomponent membrane bilayer. From the MD trajectory analyses, we have obtained the salient structural features of the α-Syn mutants. The RMSD and RMSF profiles of α-Syn mutants exhibit structural rigidity and flexibility among the varied mutants of α-Syn protein. The percentage of secondary structural content of the α-Syn mutants was calculated to be the highest in H50Q α-Syn mutant (44.1%) as compared to other mutants. In order to estimate the impact of mutation on the binding affinity of α-Syn to the lipid membrane, we have determined the number inter-molecular hydrogen bond analysis between the α-Syn and lipid membrane. The distance analysis between the N-terminal and C-terminal of α-Syn mutants showed the degree of close proximity in the α-Syn mutants that suggested the stability of the conformational structure. The conformational snapshots of the α-Syn mutants gave us insights into the effects of mutation on the membrane binding and conformational dynamics of α-Syn protein during the MD simulation time period. This study provides us the comparative details of the effects of α-Syn mutants on the membrane protein interaction.

7.2. Introduction:

In 1990, PD was linked to genetics for the first time when members of the Contursi Kindred, an Italian-American family, were discovered to have inherited early onset PD. After autopsy, studies later discovered LB pathology [468], and the α-Syn gene (SNCA) on chromosome four was the site of the causal mutation causing familial early on-set PD [2]. PD instances with an early beginning in families have been linked to α-Syn gene duplication and triplication, whereas missense point mutations of the N-terminal (A30P, A53E, A53T, E46K, H50Q, and G51D) have been substantially associated with the autosomal dominant type of the disease. Although mutant α-Syn proteins differ in a small number of amino acid residues, their shape and the kind of aggregates they produce are significantly altered [469]. It has been demonstrated that the mutant α-Syn protein (A30P and A53T disease mutations) linked to familial PD is physically

flawed for membrane binding, changing the protein's binding characteristics [153]. At the earliest possible stage, G51D is the most powerful mutation currently known to cause the illness to manifest. Even while every single alteration in an amino acid causes PD to manifest earlier, the impact they have on the pace of α-Syn aggregation and the oligomers that form are quite diverse. An enhanced rate of fibril formation, for example, is caused by the mutations A53T [2], H50Q [470], and E46K [471], whereas the mutations G51D [156], A30P [472], and A53E [473] seem to reduce the pace of fibril formation. Reduced phospholipid binding is usually the outcome of mutations, as can be observed in the G51D, A30P [156, 474], and A53E [473] variations. On the contrary, phospholipid binding is enhanced by E46K and A53T [475]. H50Q mutation enhances α-Syn aggregation with a slight effect on the lipid-binding property but is otherwise unchanged in the A53T mutation as similar in the WT. The findings imply a functional connection between α-Syn and lipid binding that may be undermined by structural and interaction alterations in early onset mutants [476]. Overexpression of A53T and E46K, which maintain the affinity for membrane binding [15, 477], interferes with the release of the transmitter [478], in contrast to A30P. The synaptic vesicle dynamics are influenced by the N-terminal of α-Syn membrane-binding domain feature. *In vitro*, when membranes are absent, the A53T and E46K mutations have a tendency to merge and create prominent twisted fibrils [475]. Experimentally, A30P showed decreased distribution in Mitochondria-associated endoplasmic reticulum membranes as a consequence of its lower affinity towards the membrane, whereas A53T demonstrated a reduction in both membrane binding and total protein production compared with the WT [479]. The A53T and A30P mutations are located in the repetitive region of the protein. The molecular pathogenetic basis is unclear, although it is likely that the mutant filamentous α-Syn performs unique activities [480]. Substituting His with Gln eliminates the imidazole's positive charge at physiological pH, preventing the creation of a stabilising salt bridge with E57 on the neighbouring filament. It also removes a possible intramolecular salt bridge with K45, which stabilises Greek key production [481].
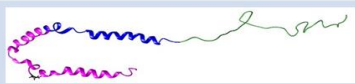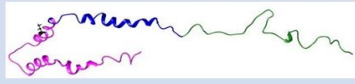
Our work provides a structural view to the PD familial mutants (A30P, A53E, A53T, E46K, H50Q, and G51D) of α-Syn and highlights the effect of mutation on the protein membrane interaction using MD simulation study. In this comparative study of the α-Syn mutants, we have determined the order of their ability in adapting to the biological membranes and the rate of change in the conformation of the α-Syn mutant in the membrane bound state.

7.3. Materials and Methods:

7.3.1. Construction of α-Synuclein mutants:

The mutations of α-Syn (A30P, A53E, A53T, E46K, G51D and H50Q) were obtained by altering the human micelle WT α-Syn residues using CHIMERA software. The alanine residue at 30th position is replaced by proline; similarly alanine at 53th position is replaced by glutamic acid and threonine. Glycine is replaced by alanine at 51th position. At 50th position, histidine is replaced by glutamine. The list of mutations of WT α-Syn protein were listed in **Table 7.1**.The construction of α-Syn mutant was discussed in section **6.3.1**.

Table 7.1. *List of mutation of α-Syn protein and its structure*

MUTATION SITE	STRUCTURE
Alanine (A) at 30 → Proline (P)	
Alanine (A) at 53 → Glutamate (E)	
Alanine (A) at 53 → Threonine (T)	
Glutamate (E) at 46 → Lysine (K)	
Glycine (G) at 51 → Aspartic acid (D)	
Histidine (H) at 50 → Glutamine (Q)	

7.3.2. Preparation of α-Synuclein mutants and lipid membrane complex:

Followed by construction of α-Syn mutants and building a membrane bound α-Syn mutants (A30P, A53E, A53T, E46K, G51D and H50Q) using CHARMM-GUI server. The methodology used to initiate the placement of α-Syn mutant on the membrane bilayer (DOPE/DOPS/DOPC in 5:3:2 ratio) was discussed in details in the section **4.3.1**.

7.3.3. MD simulation setup:

The initial orientation of the membrane bound α-Syn mutants were placed to determine the water-lipid interface using CHARMM-GUI. The MD simulation was carried out for 100 ns time period using a standard protocol as discussed in section **4.3.2.**

7.3.4. MD trajectory analysis:

To characterize the membrane bilayer, we calculated the area per lipid layer, membrane thickness and electron density profile analysis. To examine the structural stability and flexibility of the α-Syn mutants, RMSD and RMSF profile were analysed. The conformational snapshots of α-Syn mutants were obtained from the MD trajectories using CHIMERA tool. The hydrogen bond analysis between α-Syn mutant and lipid membrane were analysed. The percentage of secondary structural content using YASARA software tool and DSSP plot. The plotting were performed using xmgrace tool.

7.4. Results and Discussions:

7.4.1. Area per lipid analysis:

Area per lipid analysis determines the degree of binding to other membrane properties, acyl chain ordering, compressibility, and molecular packaging. The area per lipid of the membrane-aqueous interface are particularly crucial for verifying the accuracy of MD simulations of bio membranes and lipid bilayers. The average upper lipid layer profile of mutant A30P α-Syn showed the highest equilibrium of insertion 66.87 $Å^2$ of the protein into the lipid profile as compared to A53E (66.72 $Å^2$), A53T (66.47 $Å^2$), E46K (66.76 $Å^2$), G51D (66.84 $Å^2$) and H50Q (66.68 $Å^2$) respectively as shown in **Figure 7.1**. Similarly, the average lower lipid layer of α-Syn mutants showed highest insertion of A30P α-Syn (69.44 $Å^2$) into the lipid membrane as compared to the lower degree of insertion of A53E (69.28 $Å^2$), A53T (69.02 $Å^2$), E46K (69.33 $Å^2$), G51D (69.41 $Å^2$) and H50Q (69.25 $Å^2$) into the membrane respectively. At the interface between the water and lipid heads areas, the lateral pressure rises as it approaches the membrane and generates the positive peak.
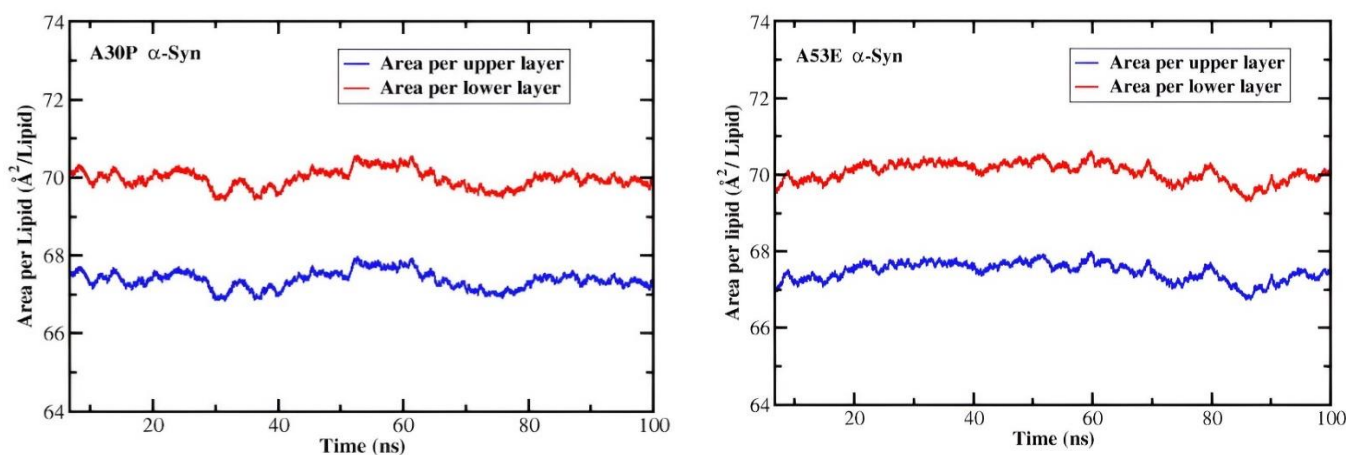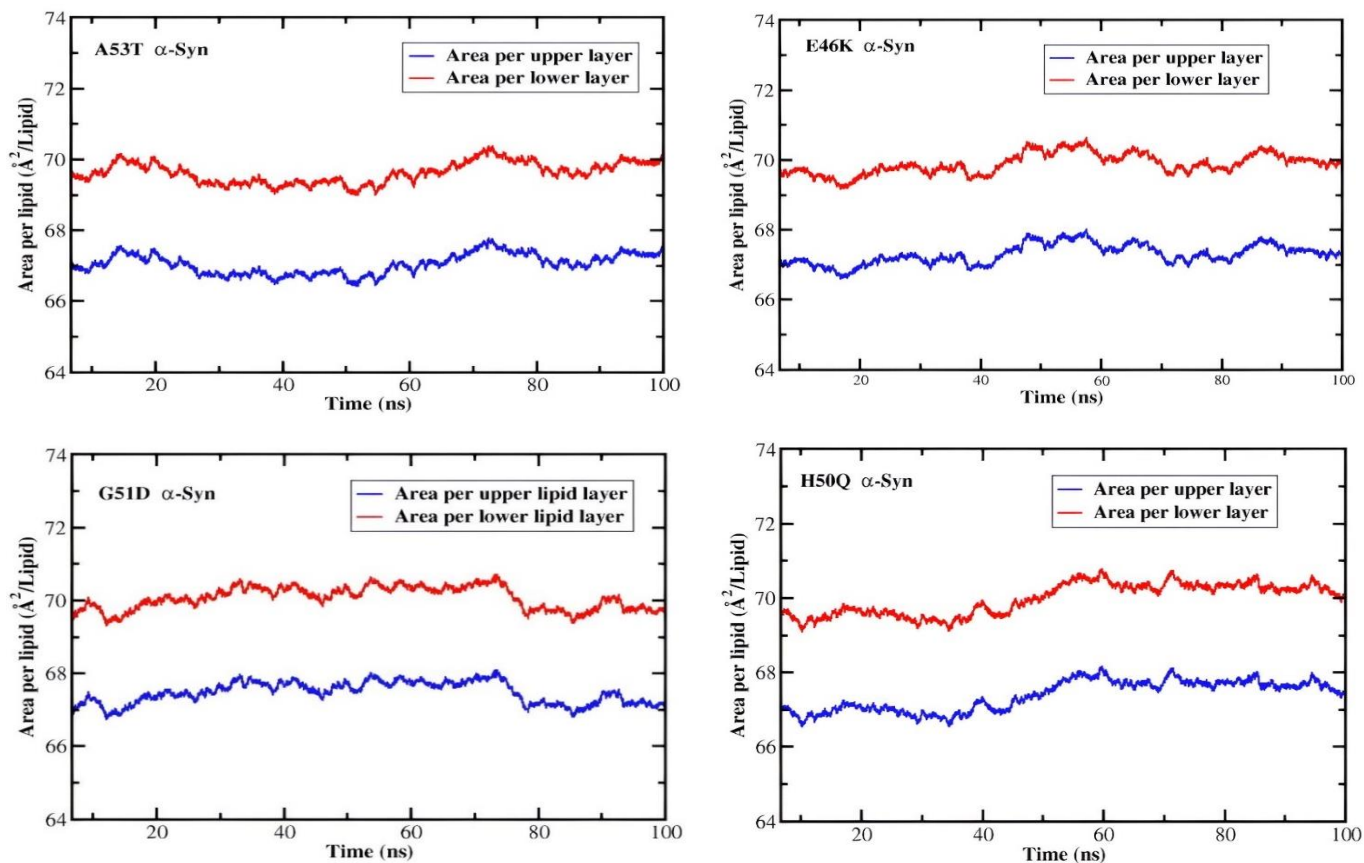
Figure 7.1. Area per lipid analysis of A30P, A53E, A53T, E46K, G51D and H50Q α-Syn mutants

7.4.2. Membrane thickness analysis:

The membrane thickness is one of the important parameters to determine the permeability of the membrane during the transition of membrane from ordered-liquid state to disordered-liquid state. In this study we have calculated the membrane thickness between the phosphate atom of upper leaflet and the other phosphate atoms present in lower leaflet as shown in **Figure 7.2**. The average membrane thickness was found to be highest in H50Q α-Syn mutant followed by A30P α-Syn, A53E α-Syn, A53T α-Syn, E46K α-Syn and G51D α-Syn respectively. The increase in membrane thickness suggests higher free energy profiles and long phospholipid chains [482]. Therefore, in the H50Q α-Syn due to higher membrane thickness there is significant net change in the position of the membrane interface with the water.
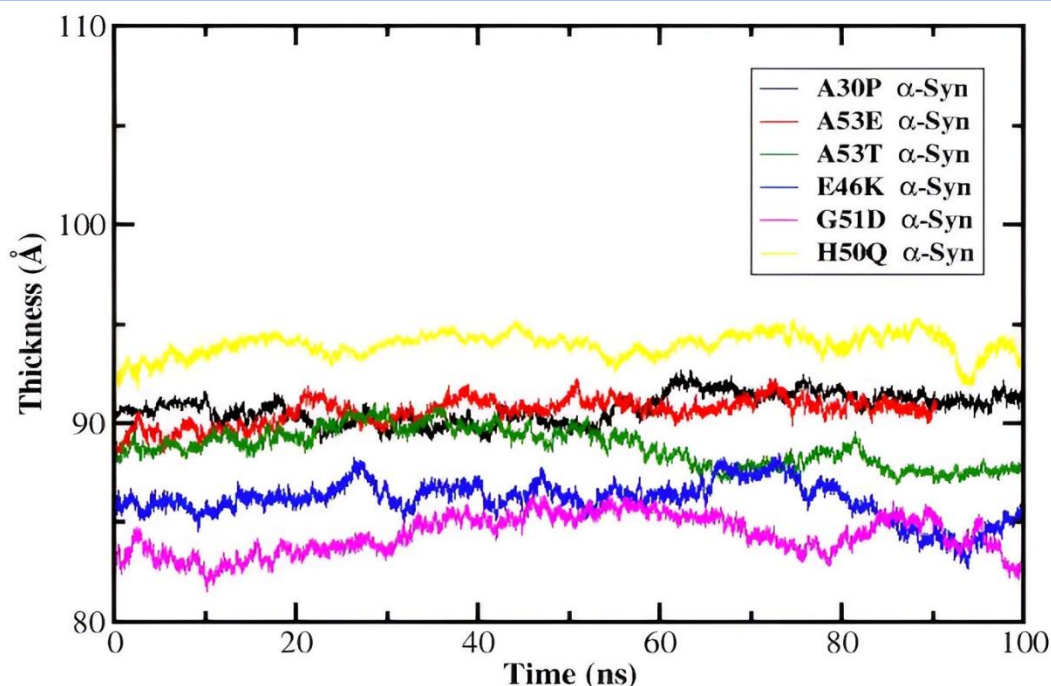
Figure 7.2. *Membrane thickness analysis of membrane bound α-Syn mutants as a function of simulation time*

7.4.3. Electron Density Profiles analysis:

The Electron density profiles provide us the detailed parameter of phospholipid bilayer membrane consists of DOPE/DOPC/DOPS in 5:3:2 ratio to determine the stabilization of membrane as shown in **Figure 7.3**. The electron density of all the membrane systems were found to be ± 20 Å that indicates stable equilibrium. In the electron density profile of all the components of the membrane systems, including oleoyl group, choline, serine and ethanolamine have showed similar density throughout the MD simulation. This is in agreement with the analysis that the membrane systems are equilibrated for further analysis.

Similarly, we have analysed the electron density profiles of different regions (N-terminal, NAC region and C-terminal) of α-Syn in membrane bound state as shown in **Figure 7.4**. From the analysis, the N-terminal of A53E α-Syn showed highest insertion of 32 Å, NAC region of A30P α-Syn showed highest insertion of 12 Å and C-terminal of E46K α-Syn showed highest insertion of 10 Å. The interaction of NAC region of α-Syn and membrane facilitates the protein to retain its conformation and hinder its interaction with other potential protein in the nearby vicinity.

(A)

(B)

(C)

(D)

(E)

(F)
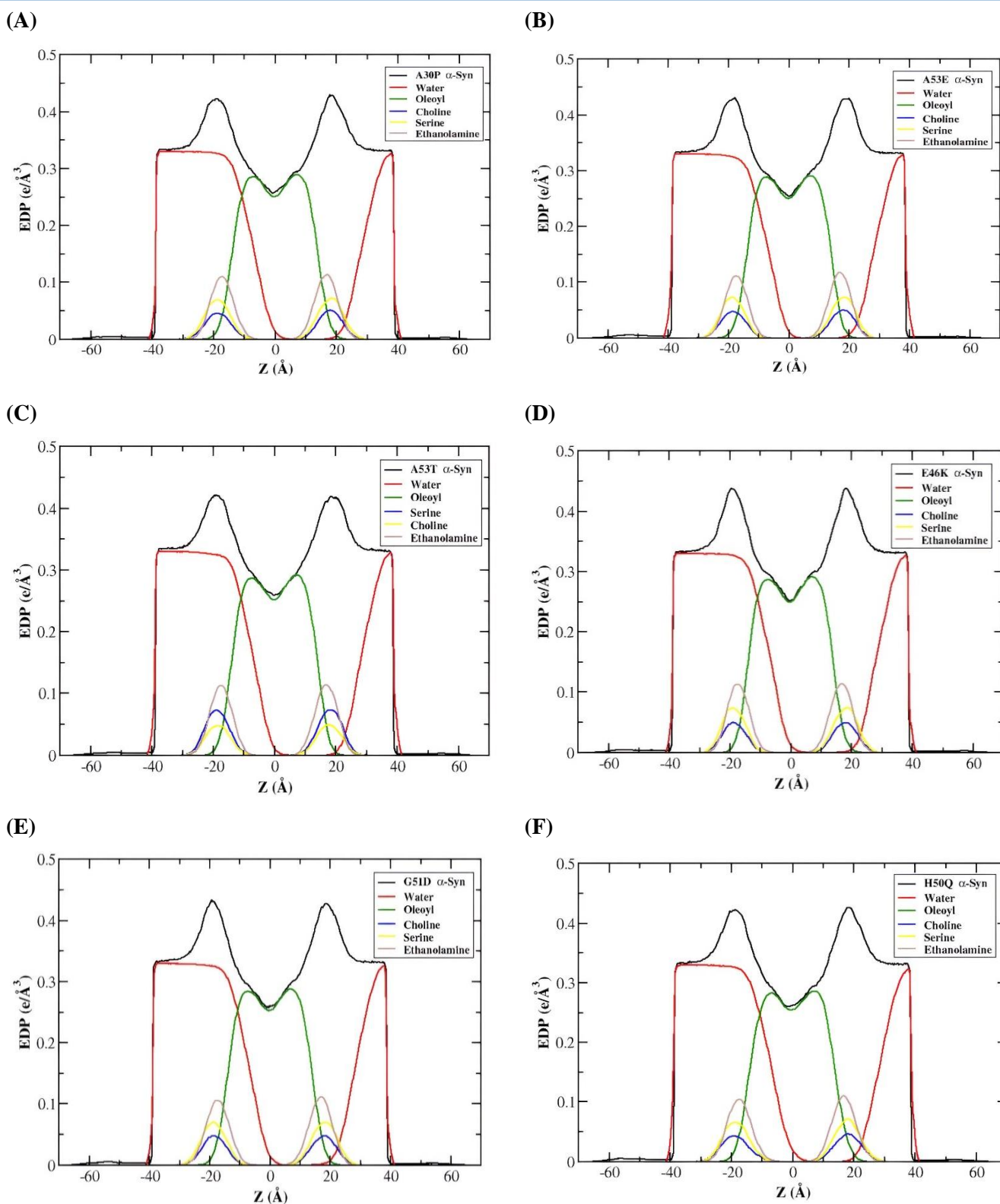
Figure 7.3. Electron density profile analysis of each component of (A) A30P, (B) A53E, (C) A53T, (D) E46K, (E) G51D and (F) H50Q α-Syn mutants

(A)

(B)

(C)

(D)

(E)

(F)
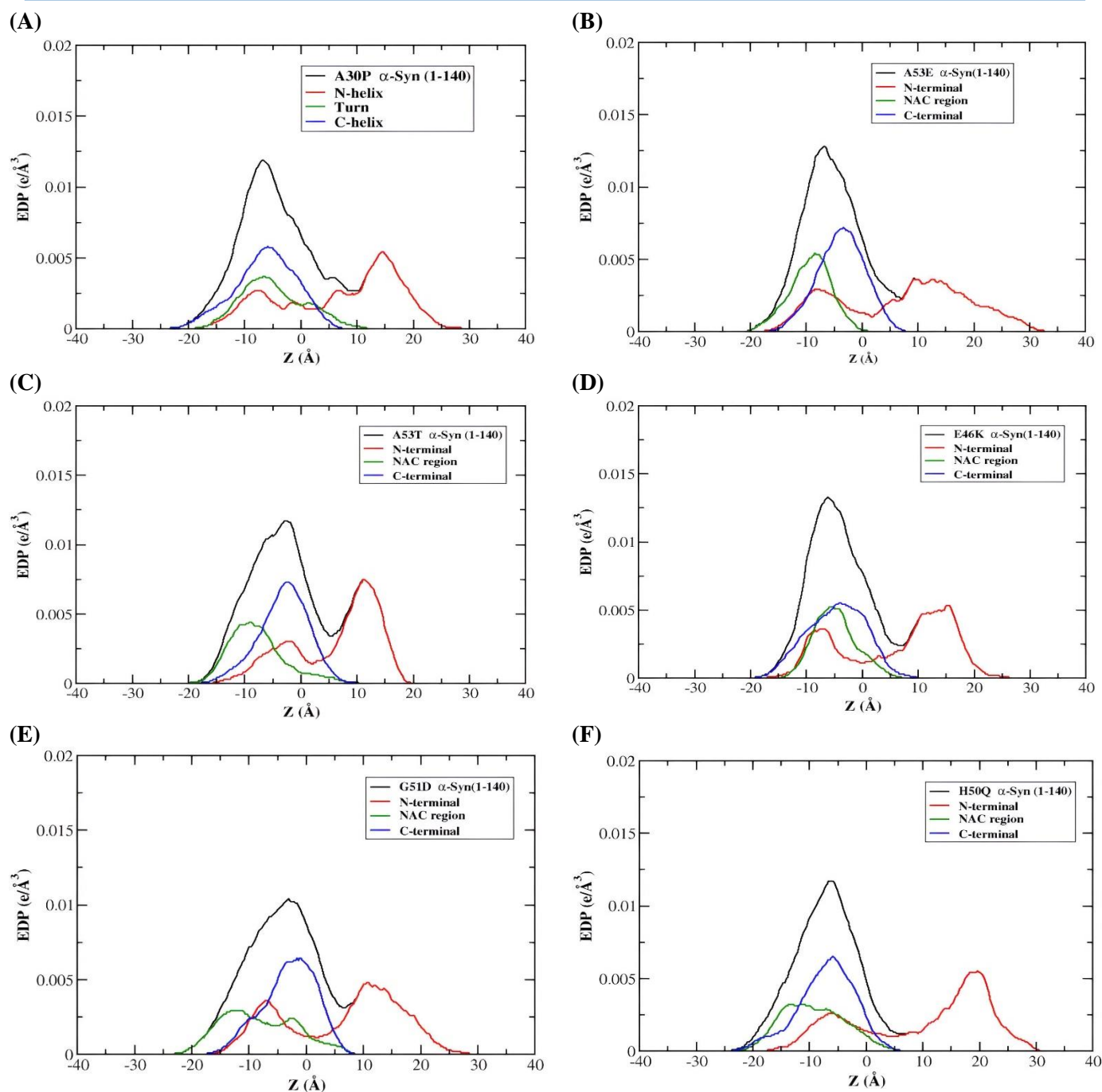
Figure 7.4. Electron density profile analysis of different regions of (A) A30P, (B) A53E, (C) A53T, (D) E46K, (E) G51D and (F) H50Q α-Syn mutants

7.4.4. RMSD analysis:

To quantify the change in α-Syn protein's backbone from its starting structural conformation to its final position, one can use the root mean square deviation, or RMSD. The variations generated throughout the simulation process can be used to assess the stability of the protein with respect to its structure. For all the α-Syn mutant complex systems studied here, the RMSD values as a function of simulation time period as shown in **Figure 7.5.** In **Figure 7.5**, a

comparative analysis was observed to have showed higher flexibility of 6.5 Å in the case of A53E α-Syn. Among all the mutants of α-Syn, E46K mutant was found to have RMSD value of 4.8 Å that suggested the structure of the α-Syn was retained throughout the MD simulation time period of 100 ns. Therefore, it was observed from the RMSD values that E46K mutant is the most rigid and stable in its conformation.
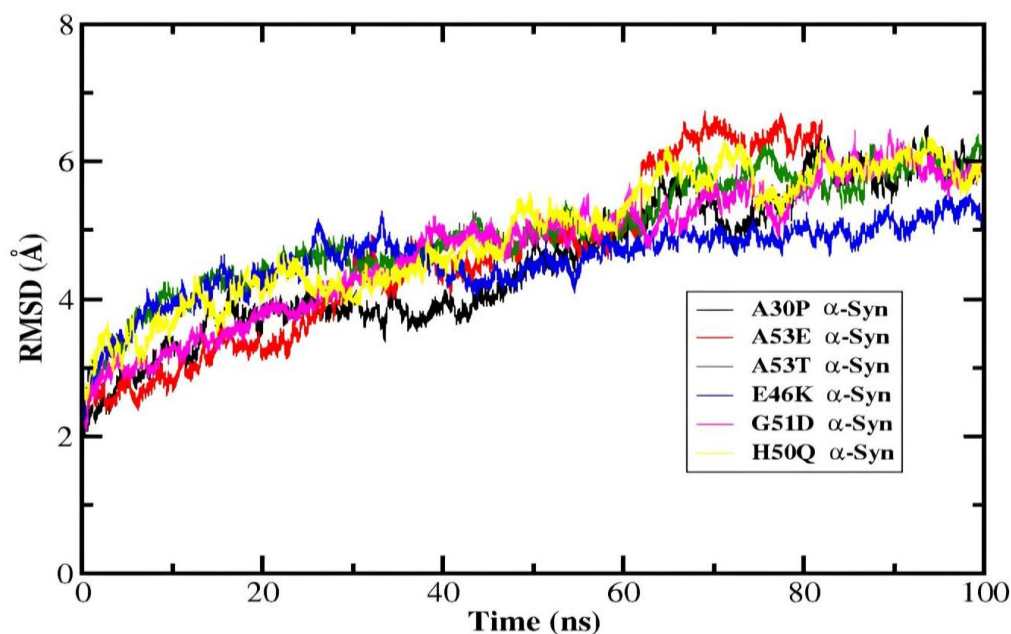
Figure 7.5. RMSD analysis of membrane bound α-Syn mutants as a function of simulation time

7.4.5. RMSF analysis:

The RMSF values of all the Cα-atoms referenced to their starting structures of the three monomer systems were determined to assess individual residue flexibility during the simulation time. **Figure 7.6** depicts the RMSF calculated with respect to time period for the α-Syn mutants. The RMSF analysis helped us to understand the fluctuation of the residues of the three systems. From **Figure 7.6**, it was observed that the residues of the E46K α-Syn mutant followed by A53E α-Syn and A30P α-Syn had overall less fluctuation. The higher fluctuation of the residues were observed in the A53T α-Syn and G51D α-Syn. Therefore, the RMSF values were found to be in conformation with the RMSD values.
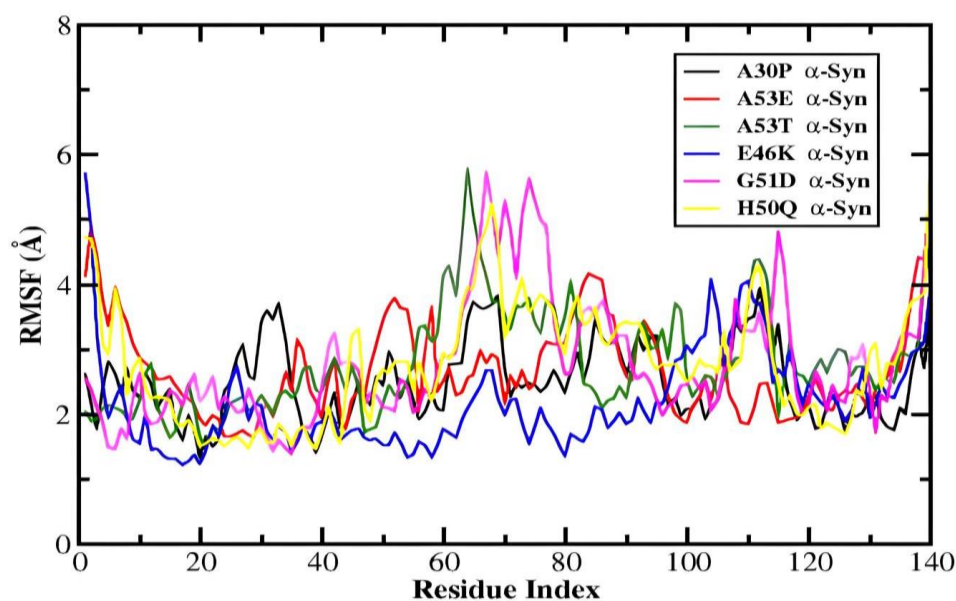
Figure 7.6. *RMSF analysis of membrane bound α-Syn mutants as a function of simulation time*

7.4.6. Intermolecular Hydrogen bond analysis:

The hydrogen bond analysis of the lipid membrane and α-Syn mutant of the overall structure is shown in **Figure 7.7**. Compared to other mutants, the overall number of intermolecular hydrogen bonds found in the H50Q α-Syn mutant is reported to decrease. The average number of inter-molecular hydrogen bonds was calculated to be 22 which is highest in the case of mutants A53T and G51D α-Syn. Also, a comparative higher number of 21 inter-molecular hydrogen bonds were observed in A53E and E46K α-Syn mutant. A lower average number of inter-molecular hydrogen bonds was observed to be 17 in the case of H50Q α-Syn. The inter-molecular hydrogen bonds between membrane bilayer as donor/acceptor and α-Syn protein as donor/acceptor. Therefore, the number of inter-molecular hydrogen bonds in H50Q α-Syn was observed to be lower than other mutants. The Inter-molecular Hydrogen bond analysis of membrane bound α-Syn mutants (A30P, A53E, A53T, E46K, G51D and H50Q) complexes during the MD simulation of 100 ns with membrane bilayer as acceptor/donor and α-Syn mutants as donor/acceptor as tabulated in **Table 7.2-7.13**.

(A)

(B)

(C)

(D)

(E)

(F)
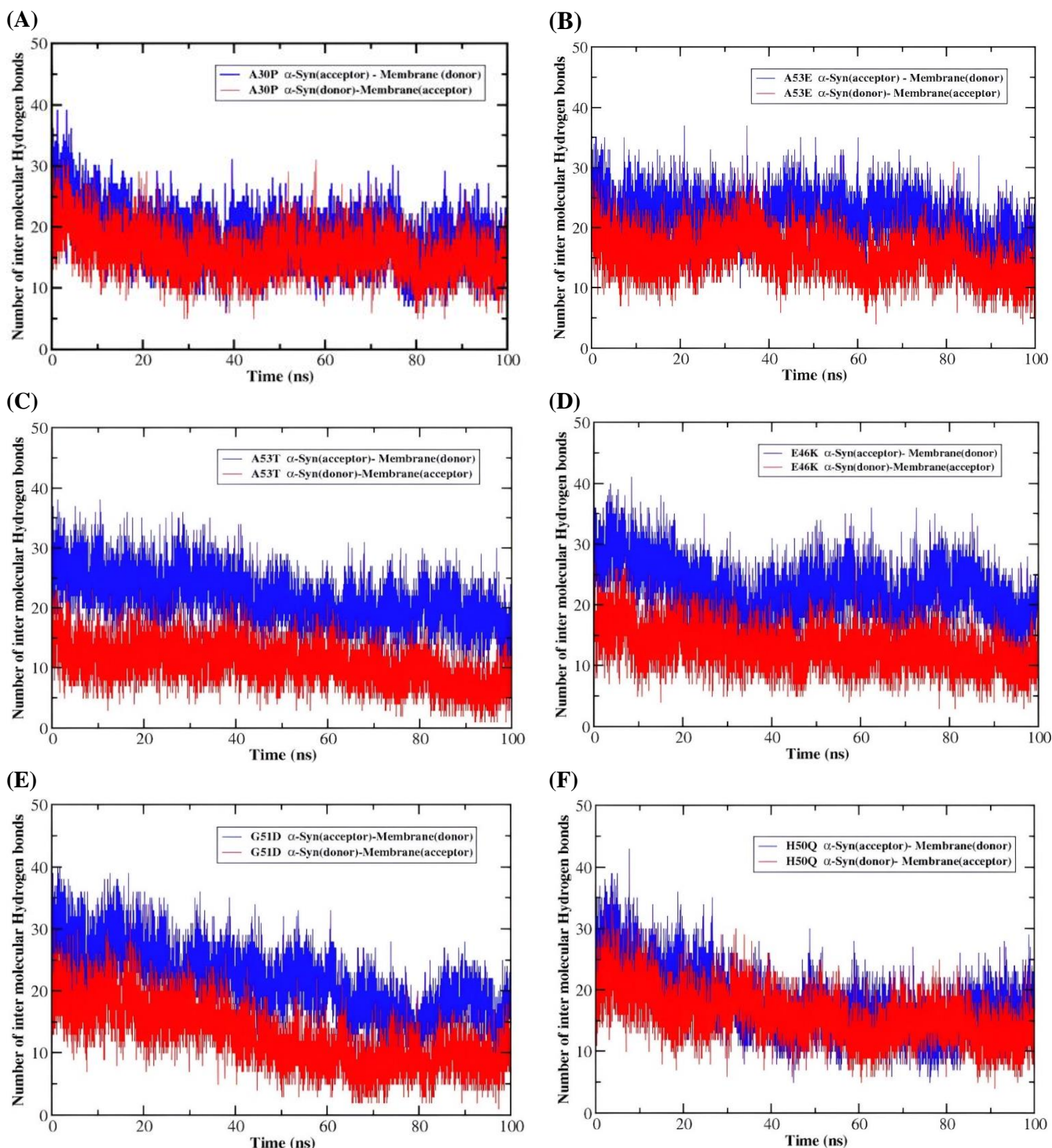
Figure 7.7. *Intermolecular Hydrogen bond analysis between (A) A30P, (B) A53E, (C) A53T, (D) E46K, (E) G51D and (F) H50Q α-Syn mutants and lipid membrane*

Table 7.2. *Intermolecular Hydrogen bond analysis of membrane bound A30P α-Syn complex during the MD simulation of 100 ns with membrane bilayer as acceptor and A30P α-Syn as donor*

#Acceptor	DonorH	Donor	Average Distance (Å)	Average Angle (º)
PE_1879@O12	LYS_10@HZ3	LYS_10@NZ	2.7823	153.813
PE_1795@O12	GLY_101@H	GLY_101@N	2.8346	156.4779
PE_1795@O34	ASN_103@HD22	ASN_103@ND2	2.8069	159.9951

PE_1870@O33	LYS_80@HZ1	LYS_80@NZ	2.7146	158.4338
PE_1870@O33	LYS_80@HZ3	LYS_80@NZ	2.7184	158.8804
PE_1786@O34	LYS_45@HZ2	LYS_45@NZ	2.7686	158.8404
PE_1867@O34	LYS_45@HZ3	LYS_45@NZ	2.7566	158.3462
PE_1786@O34	LYS_45@HZ3	LYS_45@NZ	2.7788	157.5297
PE_1831@O12	LYS_21@HZ3	LYS_21@NZ	2.7711	156.2979
PE_1867@O34	LYS_45@HZ1	LYS_45@NZ	2.7714	156.987
PE_1879@O12	LYS_10@HZ2	LYS_10@NZ	2.7855	153.6455
PE_1786@O34	LYS_45@HZ1	LYS_45@NZ	2.777	157.2244
PE_1879@O12	LYS_10@HZ1	LYS_10@NZ	2.7804	154.8031
PE_1858@O33	SER_42@HG	SER_42@OG	2.6583	163.1772
PE_1867@O34	LYS_45@HZ2	LYS_45@NZ	2.7657	158.2384
PE_1819@O34	LYS_102@HZ2	LYS_102@NZ	2.7593	158.6014
PE_1819@O34	LYS_102@HZ3	LYS_102@NZ	2.7552	159.163
PC_1873@O33	LYS_96@HZ1	LYS_96@NZ	2.7538	157.7131
PE_1870@O33	LYS_80@HZ2	LYS_80@NZ	2.7151	158.8906
PC_1825@O34	THR_92@HG1	THR_92@OG1	2.6973	163.5287
PC_1873@O33	LYS_96@HZ3	LYS_96@NZ	2.7615	157.2414
PC_1873@O33	LYS_96@HZ2	LYS_96@NZ	2.7516	157.3652
PE_1831@O12	LYS_21@HZ1	LYS_21@NZ	2.7751	155.0518
PE_1831@O12	LYS_21@HZ2	LYS_21@NZ	2.7779	155.1655
PS_151@O12	LYS_6@HZ2	LYS_6@NZ	2.7756	155.4863
PE_1822@O12	LYS_80@HZ2	LYS_80@NZ	2.7729	152.0901
PE_1795@O31	ASN_103@HD22	ASN_103@ND2	2.8778	159.2524
PE_1765@O22	LYS_80@HZ2	LYS_80@NZ	2.7692	151.799
OL_1766@H5S	VAL_3@H	VAL_3@N	2.767	151.9276
PS_175@O33	LYS_12@HZ3	LYS_12@NZ	2.7549	157.3868
PS_151@O12	LYS_6@HZ3	LYS_6@NZ	2.778	155.2026
PE_1819@O34	LYS_102@HZ1	LYS_102@NZ	2.7439	158.4085
PS_151@O22	LYS_6@HZ3	LYS_6@NZ	2.7567	156.8802
PE_1867@O33	LYS_45@HZ3	LYS_45@NZ	2.7661	158.1186
PS_1888@O33	GLN_62@HE21	GLN_62@NE2	2.7868	158.3914
PS_175@O33	LYS_12@HZ2	LYS_12@NZ	2.7544	156.3121
PE_1834@O33	LYS_32@HZ1	LYS_32@NZ	2.7559	159.9328
PS_151@O12	LYS_6@HZ1	LYS_6@NZ	2.7858	154.851
PS_1768@O12	SER_87@HG	SER_87@OG	2.6465	163.2383
PE_1840@O12	GLN_24@HE22	GLN_24@NE2	2.8429	157.3736
PE_1834@O33	LYS_32@HZ2	LYS_32@NZ	2.7686	159.0629
PE_160@O12	LYS_12@HZ3	LYS_12@NZ	2.7638	159.0253
PE_1867@O33	LYS_45@HZ2	LYS_45@NZ	2.7907	158.5459
PE_1867@O33	LYS_45@HZ1	LYS_45@NZ	2.7807	157.9035
PE_1798@O22	LYS_80@HZ1	LYS_80@NZ	2.7908	153.1912
PE_1765@O22	LYS_80@HZ3	LYS_80@NZ	2.7759	151.6716
PE_1840@O12	LYS_21@HZ2	LYS_21@NZ	2.761	154.0872
PE_1840@O12	LYS_21@HZ3	LYS_21@NZ	2.7842	152.2605
PE_1828@O12	GLU_139@H	GLU_139@N	2.8644	162.96
PE_1951@O33	THR_92@HG1	THR_92@OG1	2.6438	165.0211

Table 7.3. Intermolecular Hydrogen bond analysis of membrane bound A30P α-Syn complex during the MD simulation of 100 ns with A30P α-Syn as acceptor and membrane bilayer as donor

#Acceptor	DonorH	Donor	Average Distance (Å)	Average Angle (º)
ASP_121@OD2	PE_1801@HN1A	PE_1801@N31	2.792	156.9152
ASP_115@O	PE_1852@HN1C	PE_1852@N31	2.7887	151.0292
GLU_137@OE2	PE_1777@HN1B	PE_1777@N31	2.7563	158.0135
ASP_121@OD2	PE_1801@HN1C	PE_1801@N31	2.7791	158.0551
ASP_121@OD2	PE_1801@HN1B	PE_1801@N31	2.787	157.5903
GLU_105@OE2	PE_1861@HN1B	PE_1861@N31	2.8066	155.1078
GLU_130@OE2	PE_1849@HN1C	PE_1849@N31	2.777	157.1998
GLU_137@OE2	PE_1777@HN1C	PE_1777@N31	2.7612	156.9634

ASP_121@OD1	PE_1801@HN1A	PE_1801@N31	2.8216	152.0435
GLU_131@OE1	PE_1849@HN1B	PE_1849@N31	2.771	159.7248
ASP_115@O	PE_1852@HN1B	PE_1852@N31	2.7876	152.8388
GLU_137@OE2	PE_1777@HN1A	PE_1777@N31	2.7557	155.8723
GLU_139@OE2	PE_2515@HN1A	PE_2515@N31	2.8108	154.743
ASP_115@OD2	PE_1900@HN1A	PE_1900@N31	2.7762	155.4132
GLU_139@OE1	PE_2515@HN1A	PE_2515@N31	2.7939	154.0016
GLU_105@OE1	PE_1861@HN1C	PE_1861@N31	2.8002	154.9946
ASP_119@OD2	PE_1816@HN1B	PE_1816@N31	2.7936	156.9565
ASP_115@OD2	PE_1900@HN1C	PE_1900@N31	2.7752	155.1009
ASP_119@OD2	PE_1816@HN1C	PE_1816@N31	2.7782	157.724
GLU_105@OE2	PE_1861@HN1C	PE_1861@N31	2.8018	154.2468
GLU_130@OE2	PE_1849@HN1A	PE_1849@N31	2.7759	152.9283
ASP_135@OD2	PE_1771@HN1B	PE_1771@N31	2.79	156.3269
GLU_139@OE1	PE_2515@HN1B	PE_2515@N31	2.7991	152.7172
GLU_105@OE1	PE_1861@HN1B	PE_1861@N31	2.8021	152.8287
GLU_139@OE2	PE_2515@HN1B	PE_2515@N31	2.8159	153.7805
GLU_105@OE1	PE_1861@HN1A	PE_1861@N31	2.7895	154.2434
ASP_119@OD1	PE_1801@HN1B	PE_1801@N31	2.8012	159.8361
GLU_114@OE2	PE_1876@HN1C	PE_1876@N31	2.7911	157.7569
GLU_126@OE1	PE_1777@HN1C	PE_1777@N31	2.8124	153.8865
ASP_119@OD2	PE_1816@HN1A	PE_1816@N31	2.7808	157.4427
ASP_135@OD2	PE_1771@HN1A	PE_1771@N31	2.7859	156.4775
GLU_104@OE2	PE_1948@HN1C	PE_1948@N31	2.7933	160.1288
GLU_104@OE2	PE_1792@HN1A	PE_1792@N31	2.7887	155.3851
VAL_3@H	OL_1766@H5S	OL_1766@C15	2.8017	150.4519
GLU_105@OE2	PE_1861@HN1A	PE_1861@N31	2.8087	154.4072
GLU_139@OE2	PE_2515@HN1C	PE_2515@N31	2.8186	155.4098
ASP_135@OD1	PS_1804@HN1B	PS_1804@N31	2.8116	158.6999
GLU_131@OE1	PE_1933@HN1B	PE_1933@N31	2.8057	156.3283
GLU_104@OE2	PE_1792@HN1C	PE_1792@N31	2.7832	155.4685
GLU_131@OE1	PE_1849@HN1C	PE_1849@N31	2.7783	158.5772
GLU_83@OE1	PE_1870@HN1A	PE_1870@N31	2.7863	155.337
GLU_139@OE1	PE_2515@HN1C	PE_2515@N31	2.7953	152.0796
ASP_121@OD1	PE_1801@HN1B	PE_1801@N31	2.7883	155.139
GLU_104@OE1	PE_1792@HN1A	PE_1792@N31	2.7884	157.2664
GLU_123@OE2	PE_1810@HN1A	PE_1810@N31	2.7952	156.198
GLU_104@OE1	PE_1792@HN1B	PE_1792@N31	2.7882	157.0122
GLU_83@OE1	PE_1870@HN1C	PE_1870@N31	2.7867	155.3226
GLU_131@OE2	PE_1849@HN1A	PE_1849@N31	2.7806	158.6746
GLU_83@OE1	PE_1870@HN1B	PE_1870@N31	2.7891	153.6969

Table 7.4. Intermolecular Hydrogen bond analysis of membrane bound A53E α-Syn complex during the MD simulation of 100 ns with membrane bilayer as acceptor and A53E α-Syn as donor

#Acceptor	DonorH	Donor	Average Distance (Å)	Average Angle (º)
PE_1837@O12	ASP_98@H	ASP_98@N	2.825	163.4502
PS_1894@O33	GLN_109@HE21	GLN_109@NE2	2.7969	162.1975
PC_1762@O22	LYS_102@H	LYS_102@N	2.8156	149.1622
PE_1834@O12	GLN_24@HE22	GLN_24@NE2	2.8184	158.6313
PS_1771@O35	THR_72@HG1	THR_72@OG1	2.6446	163.8428
PE_1822@O34	ASN_103@HD22	ASN_103@ND2	2.793	161.8111
PS_1870@O22	TYR_133@HH	TYR_133@OH	2.7018	163.372
PC_1873@O22	TYR_133@HH	TYR_133@OH	2.714	159.2651
PE_1765@O34	GLN_134@HE22	GLN_134@NE2	2.8176	153.8481
PE_1795@O22	LYS_45@H	LYS_45@N	2.8314	162.7127
PS_1783@O33	LYS_97@HZ1	LYS_97@NZ	2.7832	157.6962
PS_1771@O35	THR_72@H	THR_72@N	2.8303	151.5317
PS_1783@O22	LYS_97@HZ3	LYS_97@NZ	2.7512	156.0924
PE_1915@O34	LYS_80@HZ2	LYS_80@NZ	2.7671	157.9335

PE_1861@O33	LYS_80@HZ1	LYS_80@NZ	2.7538	160.6461
PE_1861@O22	LYS_80@HZ3	LYS_80@NZ	2.763	159.0676
PS_181@O34	LYS_6@HZ3	LYS_6@NZ	2.7425	158.3049
PE_1861@O22	LYS_80@HZ2	LYS_80@NZ	2.7717	156.9359
PE_1792@O34	LYS_58@HZ1	LYS_58@NZ	2.7532	159.2386
PS_1840@O12	SER_42@H	SER_42@N	2.8633	160.1896
PE_1861@O33	LYS_80@HZ2	LYS_80@NZ	2.7633	159.9799
PS_181@O34	LYS_6@HZ1	LYS_6@NZ	2.7668	158.4513
PS_1771@O36	GLY_73@H	GLY_73@N	2.8588	161.8696
PE_1822@O33	LYS_102@HZ2	LYS_102@NZ	2.7483	158.5281
PE_1900@O34	SER_87@HG	SER_87@OG	2.6358	163.3692
PE_1915@O34	LYS_80@HZ1	LYS_80@NZ	2.7824	158.4678
PE_1816@O22	LYS_32@HZ2	LYS_32@NZ	2.765	154.7666
PE_1816@O22	LYS_32@HZ3	LYS_32@NZ	2.7661	155.4666
PE_1780@O12	LYS_34@HZ1	LYS_34@NZ	2.7669	156.2764
PS_1783@O22	LYS_97@HZ1	LYS_97@NZ	2.7594	155.7061
PS_1840@O33	SER_42@HG	SER_42@OG	2.6143	164.0762
PE_1822@O33	LYS_102@HZ1	LYS_102@NZ	2.756	158.9309
PS_1771@O36	THR_72@H	THR_72@N	2.8477	162.7173
PE_1792@O34	LYS_58@HZ3	LYS_58@NZ	2.7573	159.533
PE_1816@O22	LYS_32@HZ1	LYS_32@NZ	2.7637	154.7935
PE_1780@O12	LYS_34@HZ3	LYS_34@NZ	2.7658	157.0693
PS_1855@O12	LYS_21@HZ1	LYS_21@NZ	2.7497	153.4975
PS_1783@O33	LYS_97@HZ2	LYS_97@NZ	2.776	157.1887
PE_1822@O33	LYS_102@HZ3	LYS_102@NZ	2.7547	158.7732
PS_1849@O35	LYS_58@HZ2	LYS_58@NZ	2.7592	152.6065
PE_1822@O33	LYS_97@HZ1	LYS_97@NZ	2.7618	156.2328
PE_1861@O22	LYS_80@HZ1	LYS_80@NZ	2.7628	155.5544
PS_1783@O33	LYS_97@HZ3	LYS_97@NZ	2.7728	158.3506
PC_1762@O22	GLY_101@H	GLY_101@N	2.8308	153.79
PE_1861@O33	LYS_80@HZ3	LYS_80@NZ	2.7636	159.8366
PE_1780@O12	LYS_34@HZ2	LYS_34@NZ	2.7702	157.3928
PC_160@O12	ASP_2@H	ASP_2@N	2.8134	162.4374
PS_1849@O35	LYS_58@HZ3	LYS_58@NZ	2.749	153.2925
PS_1903@O33	LYS_58@HZ3	LYS_58@NZ	2.7889	160.0113

Table 7.5. Intermolecular Hydrogen bond analysis of membrane bound A53E α-Syn complex during the MD simulation of 100 ns with A53E α-Syn as acceptor and membrane bilayer as donor

#Acceptor	DonorH	Donor	Average Distance (Å)	Average Angle (º)
ASP_115@OD2	PS_1906@HN1A	PS_1906@N31	2.7572	154.6657
GLU_137@OE1	PE_1777@HN1A	PE_1777@N31	2.7823	159.9228
ASP_115@OD2	PS_1906@HN1C	PS_1906@N31	2.782	159.5054
GLU_137@OE1	PE_1777@HN1B	PE_1777@N31	2.7777	160.4
ASP_121@OD1	PE_1852@HN1B	PE_1852@N31	2.7865	156.3416
ASP_119@OD1	PE_1852@HN1C	PE_1852@N31	2.8192	154.706
ASP_121@OD2	PE_1852@HN1B	PE_1852@N31	2.8009	156.5605
ASP_135@OD2	PE_1765@HN1B	PE_1765@N31	2.7846	156.471
ASP_135@OD2	PE_1765@HN1A	PE_1765@N31	2.7886	155.8912
ASP_119@OD1	PE_1852@HN1A	PE_1852@N31	2.8174	156.5711
GLU_137@OE1	PE_1777@HN1C	PE_1777@N31	2.7702	158.7333
ASP_121@OD1	PE_1852@HN1C	PE_1852@N31	2.7937	156.5411
ALA_91@O	PS_1843@HN1A	PS_1843@N31	2.8154	159.0368
ASP_119@OD2	PE_1852@HN1C	PE_1852@N31	2.8266	151.0068
ASP_121@OD1	PE_1852@HN1A	PE_1852@N31	2.7938	154.3345
ASP_121@OD2	PE_1852@HN1C	PE_1852@N31	2.7994	154.5061
ASP_98@O	PE_1837@HN1B	PE_1837@N31	2.8043	153.8005
VAL_70@O	PS_1771@HN1A	PS_1771@N31	2.8129	153.4814
ASP_115@OD2	PS_1906@HN1B	PS_1906@N31	2.819	152.4478
ASP_135@OD2	PE_1765@HN1C	PE_1765@N31	2.7919	153.6337

ALA_91@O	PS_1843@HN1B	PS_1843@N31	2.8056	157.6489
ASP_115@OD1	PS_1906@HN1B	PS_1906@N31	2.8433	153.0718
ASP_135@O	PE_1765@HN1B	PE_1765@N31	2.829	151.9604
ASP_119@OD1	PE_1852@HN1B	PE_1852@N31	2.8193	154.3309
THR_92@OG1	PS_1843@HN1B	PS_1843@N31	2.8496	156.8475
ASP_98@O	PE_1837@HN1C	PE_1837@N31	2.8015	155.0851
ASP_98@OD2	PE_1837@HN1B	PE_1837@N31	2.7756	155.6143
GLU_61@OE1	PE_1912@HN1A	PE_1912@N31	2.7911	156.4732
THR_92@OG1	PS_1843@HN1A	PS_1843@N31	2.8498	156.1934
ASP_121@OD2	PE_1852@HN1A	PE_1852@N31	2.8169	152.9905
ASP_98@O	PE_1837@HN1A	PE_1837@N31	2.809	155.145
ASP_115@OD1	PS_1906@HN1C	PS_1906@N31	2.8466	152.2458
GLU_28@OE1	PE_1816@HN1B	PE_1816@N31	2.792	152.8541
GLU_114@OE1	PE_1876@HN1A	PE_1876@N31	2.7879	156.9985
GLU_61@OE2	PE_1792@HN1B	PE_1792@N31	2.786	155.8087
GLU_114@OE2	PE_1876@HN1B	PE_1876@N31	2.7934	155.6109
GLU_139@OE1	PE_1774@HN1A	PE_1774@N31	2.7999	157.8898
THR_92@OG1	PS_1843@HN1C	PS_1843@N31	2.8517	156.609
THR_59@OG1	PE_1816@HN1B	PE_1816@N31	2.8564	154.8596
ALA_91@O	PS_1843@HN1C	PS_1843@N31	2.8148	156.4546
GLU_61@OE1	PE_1912@HN1B	PE_1912@N31	2.7942	155.3853
GLN_62@OE1	PE_1816@HN1A	PE_1816@N31	2.8048	155.8351
GLU_110@OE1	PS_1906@HN1A	PS_1906@N31	2.814	159.068
THR_59@OG1	PE_1816@HN1C	PE_1816@N31	2.8547	153.1516
GLY_84@O	PE_1861@HN1A	PE_1861@N31	2.8121	151.1654
ASP_135@O	PE_1765@HN1C	PE_1765@N31	2.8266	151.9673
ASP_119@OD2	PE_1852@HN1A	PE_1852@N31	2.8346	149.832
ASP_119@OD2	PE_1852@HN1B	PE_1852@N31	2.8278	150.564
GLU_137@O	PE_1777@HN1B	PE_1777@N31	2.8226	147.1223
VAL_70@O	PS_1771@HN1C	PS_1771@N31	2.8372	157.6664

Table 7.6. *Intermolecular Hydrogen bond analysis of membrane bound A53T α-Syn complex during the MD simulation of 100 ns with membrane bilayer as acceptor and A53T α-Syn as donor*

#Acceptor	DonorH	Donor	Average Distance (Å)	Average Angle (º)
PE_1771@O22	TYR_136@HH	TYR_136@OH	2.6755	163.9783
PC_1846@O12	ASP_2@H	ASP_2@N	2.8357	147.1466
PS_1798@O35	VAL_48@H	VAL_48@N	2.8118	157.488
PE_1855@O33	LYS_102@H	LYS_102@N	2.8555	161.7287
PE_1825@O22	LYS_45@HZ1	LYS_45@NZ	2.7776	160.2612
PS_1861@O12	ASN_103@H	ASN_103@N	2.8235	158.6033
PS_1849@O33	LYS_6@HZ3	LYS_6@NZ	2.7301	159.7374
PS_2497@O12	TYR_133@HH	TYR_133@OH	2.7146	161.6599
PC_1846@O12	MET_1@H3	MET_1@N	2.7716	149.2077
PS_1819@O34	GLN_24@HE22	GLN_24@NE2	2.7905	160.9288
PS_1798@O12	LYS_43@HZ3	LYS_43@NZ	2.7782	158.0694
PS_1798@O36	LYS_43@HZ2	LYS_43@NZ	2.7384	157.7613
PS_1798@O35	GLY_47@H	GLY_47@N	2.8059	158.5157
PE_1825@O22	LYS_45@HZ3	LYS_45@NZ	2.7803	160.2083
PE_1825@O22	LYS_45@HZ2	LYS_45@NZ	2.773	160.1214
PC_1882@O22	VAL_95@H	VAL_95@N	2.8276	159.0738
PC_1846@O12	MET_1@H1	MET_1@N	2.7732	149.2473
PC_1846@O33	LYS_80@HZ2	LYS_80@NZ	2.7726	161.9643
PC_1846@O12	MET_1@H2	MET_1@N	2.7715	149.2488
PE_1825@O34	LYS_45@HZ2	LYS_45@NZ	2.7933	160.0621
PS_1798@O35	VAL_49@H	VAL_49@N	2.8614	164.7316
PS_1849@O33	LYS_6@HZ2	LYS_6@NZ	2.7474	156.712
PS_1807@O34	LYS_45@HZ3	LYS_45@NZ	2.7487	158.2193
PC_1846@O33	LYS_80@HZ1	LYS_80@NZ	2.7641	159.9487
PS_1798@O36	GLY_47@H	GLY_47@N	2.7959	161.2545

PE_1825@O34	LYS_45@HZ1	LYS_45@NZ	2.7943	160.4605
PS_1807@O33	LYS_45@H	LYS_45@N	2.8588	161.5604
PS_1903@O34	LYS_45@HZ2	LYS_45@NZ	2.7568	158.663
PS_1765@O34	LYS_97@HZ1	LYS_97@NZ	2.7658	157.9382
PS_1849@O33	LYS_6@HZ1	LYS_6@NZ	2.743	158.4531
PE_1825@O34	LYS_45@HZ3	LYS_45@NZ	2.7892	159.546
PS_1942@O35	SER_87@HG	SER_87@OG	2.6815	161.5535
PS_1798@O36	VAL_48@H	VAL_48@N	2.8119	151.3879
PC_1846@O34	LYS_6@HZ1	LYS_6@NZ	2.776	159.6975
PS_1903@O34	LYS_45@HZ3	LYS_45@NZ	2.7417	158.3911
PS_1807@O34	LYS_45@HZ1	LYS_45@NZ	2.7441	158.5983
PE_1813@O33	LYS_80@HZ1	LYS_80@NZ	2.7628	157.3864
PC_1846@O33	LYS_80@HZ3	LYS_80@NZ	2.7803	161.3414
PC_1846@O33	LYS_6@HZ1	LYS_6@NZ	2.7613	156.3648
PE_1777@O33	SER_87@HG	SER_87@OG	2.6363	166.186
PS_1804@O12	SER_129@H	SER_129@N	2.8251	157.7931
PS_1765@O34	LYS_97@HZ3	LYS_97@NZ	2.7642	157.8204
PE_1840@O12	LYS_96@HZ2	LYS_96@NZ	2.7676	156.0993
PE_1840@O12	LYS_96@HZ1	LYS_96@NZ	2.7704	155.5703
PS_1819@O36	GLN_62@HE21	GLN_62@NE2	2.8044	160.1621
PE_1813@O33	LYS_80@HZ3	LYS_80@NZ	2.7689	155.9097
PS_1849@O12	LYS_10@HZ3	LYS_10@NZ	2.7776	155.3137
PE_1801@O12	GLN_99@HE21	GLN_99@NE2	2.8199	163.4609
PE_1840@O12	LYS_96@HZ3	LYS_96@NZ	2.768	156.1626
PS_1942@O22	MET_1@H2	MET_1@N	2.7939	151.7088

Table 7.7. *Intermolecular Hydrogen bond analysis of membrane bound A53T α-Syn complex during the MD simulation of 100 ns with A53T α-Syn as acceptor and membrane bilayer as donor*

#Acceptor	DonorH	Donor	Average Distance (Å)	Average Angle (º)
ASP_115@OD2	PE_1894@HN1C	PE_1894@N31	2.7923	156.7245
GLU_105@OE1	PE_1792@HN1A	PE_1792@N31	2.7845	157.2892
GLU_105@OE1	PE_1792@HN1C	PE_1792@N31	2.7883	158.1784
GLU_105@OE1	PE_1792@HN1B	PE_1792@N31	2.7848	156.6381
ALA_140@O	PE_1909@HN1A	PE_1909@N31	2.7984	156.0137
LYS_45@O	PS_1798@HN1B	PS_1798@N31	2.8181	153.389
LYS_45@O	PS_1798@HN1C	PS_1798@N31	2.8134	153.2711
GLU_105@OE2	PE_1792@HN1B	PE_1792@N31	2.7953	152.7787
ALA_140@O	PE_1909@HN1C	PE_1909@N31	2.7946	154.9127
ALA_140@OXT	PE_1909@HN1C	PE_1909@N31	2.791	154.6886
ASP_115@OD1	PE_1894@HN1C	PE_1894@N31	2.8142	154.5614
ALA_140@OXT	PE_1909@HN1A	PE_1909@N31	2.8081	153.6236
GLU_126@OE2	PS_1783@HN1A	PS_1783@N31	2.8022	153.6019
LYS_45@O	PS_1798@HN1A	PS_1798@N31	2.8067	153.0158
ALA_140@OXT	PE_1909@HN1B	PE_1909@N31	2.8005	155.8664
GLU_126@OE1	PS_1783@HN1C	PS_1783@N31	2.8158	155.101
GLU_126@OE2	PS_1783@HN1C	PS_1783@N31	2.808	153.4672
GLU_126@OE1	PS_1783@HN1A	PS_1783@N31	2.8152	156.3154
GLU_126@OE2	PS_1783@HN1B	PS_1783@N31	2.8046	156.2726
VAL_55@O	PS_1762@HN1C	PS_1762@N31	2.8079	155.8544
GLU_126@OE1	PS_1783@HN1B	PS_1783@N31	2.818	155.0272
VAL_55@O	PS_1762@HN1B	PS_1762@N31	2.8167	157.1374
GLU_105@OE2	PE_1792@HN1A	PE_1792@N31	2.8179	150.2384
ASP_115@OD2	PE_1894@HN1A	PE_1894@N31	2.8011	153.001
GLU_105@OE2	PE_1792@HN1C	PE_1792@N31	2.8209	150.4526
ALA_140@O	PE_1909@HN1B	PE_1909@N31	2.7918	154.0466
VAL_55@O	PS_1762@HN1A	PS_1762@N31	2.8197	154.6371
MET_116@O	PS_1789@HN1C	PS_1789@N31	2.8347	151.9281
ASP_115@OD1	PE_1894@HN1A	PE_1894@N31	2.7935	153.9924
GLU_83@OE2	PE_1912@HN1B	PE_1912@N31	2.7878	157.1038

TYR_136@HH	PE_1771@HA	PE_1771@C3	2.9292	152.025
GLU_46@HA	PS_1798@H2A	PS_1798@C32	2.8807	147.2411
ASP_115@OD1	PS_1789@HN1A	PS_1789@N31	2.8033	156.3796
ASP_115@OD2	PE_1894@HN1B	PE_1894@N31	2.8019	153.4747
GLU_83@OE1	PE_1912@HN1B	PE_1912@N31	2.7843	156.2265
GLU_83@OE1	PE_1912@HN1C	PE_1912@N31	2.7916	155.4755
LEU_100@O	PE_1855@HN1C	PE_1855@N31	2.8066	155.2023
ASP_115@O	PE_1894@HN1B	PE_1894@N31	2.8208	154.4676
MET_116@O	PS_1789@HN1B	PS_1789@N31	2.8301	151.4533
LEU_100@O	PE_1855@HN1A	PE_1855@N31	2.8131	152.4304
LEU_100@O	PE_1855@HN1B	PE_1855@N31	2.8315	153.8858
ASP_115@O	PS_1789@HN1A	PS_1789@N31	2.8407	151.3258
THR_59@OG1	PS_1762@HN1A	PS_1762@N31	2.8471	157.2873
ASP_98@O	PE_1855@HN1A	PE_1855@N31	2.805	151.3401
MET_116@O	PS_1789@HN1A	PS_1789@N31	2.8301	151.4826
GLU_83@OE2	PE_1912@HN1C	PE_1912@N31	2.7873	157.3345
ASP_115@OD1	PS_1789@HN1C	PS_1789@N31	2.8064	153.1659
ASP_98@O	PE_1855@HN1B	PE_1855@N31	2.8128	152.5666
MET_1@HA	PC_1846@HX	PC_1846@C2	2.9297	149.5808
ASP_98@O	PE_1855@HN1C	PE_1855@N31	2.8035	152.3548

Table 7.8. Intermolecular Hydrogen bond analysis of membrane bound E46K α-Syn complex during the MD simulation of 100 ns with membrane bilayer as acceptor and E46K α-Syn as donor

#Acceptor	DonorH	Donor	Average Distance (Å)	Average Angle (º)
PS_1834@O34	THR_75@HG1	THR_75@OG1	2.6172	164.7264
PS_1789@O12	TYR_39@HH	TYR_39@OH	2.7092	164.2286
PE_1879@O22	GLN_24@HE22	GLN_24@NE2	2.8259	155.4776
PE_1795@O33	LYS_80@HZ3	LYS_80@NZ	2.7519	160.6364
PC_1810@O12	GLN_134@HE22	GLN_134@NE2	2.8331	153.2312
PC_1774@O33	ALA_107@H	ALA_107@N	2.846	161.2056
PS_1834@O36	LYS_80@HZ2	LYS_80@NZ	2.7433	157.6879
PE_1870@O33	GLU_110@H	GLU_110@N	2.8178	160.2165
PE_1795@O33	LYS_80@HZ2	LYS_80@NZ	2.7557	159.9903
PE_1867@O33	LYS_80@HZ1	LYS_80@NZ	2.7552	158.6089
PE_1864@O22	GLN_109@HE22	GLN_109@NE2	2.8245	161.4927
PS_1834@O36	LYS_80@HZ1	LYS_80@NZ	2.7363	155.9619
PC_1774@O12	GLN_109@HE21	GLN_109@NE2	2.7809	160.0649
PC_1873@O33	GLN_62@HE21	GLN_62@NE2	2.7881	160.5563
PC_1762@O33	TYR_136@HH	TYR_136@OH	2.6736	162.159
PE_1828@O33	LYS_97@HZ1	LYS_97@NZ	2.7398	157.7952
PE_1828@O12	GLN_99@HE22	GLN_99@NE2	2.832	156.5935
PS_1834@O35	LYS_6@HZ2	LYS_6@NZ	2.7729	153.1341
PE_1795@O33	LYS_80@HZ1	LYS_80@NZ	2.7635	159.991
PE_1828@O33	GLN_99@HE22	GLN_99@NE2	2.7884	158.6541
PC_1858@O33	LYS_96@HZ2	LYS_96@NZ	2.7522	156.9404
PS_1834@O36	LYS_6@HZ2	LYS_6@NZ	2.777	154.5509
PS_1840@O35	LYS_32@HZ3	LYS_32@NZ	2.7742	156.5474
PE_1864@O33	ASP_115@H	ASP_115@N	2.7878	158.6984
PS_1840@O36	LYS_32@HZ3	LYS_32@NZ	2.7881	157.2283
PS_1834@O35	LYS_6@HZ1	LYS_6@NZ	2.7755	154.9094
PS_1834@O33	THR_75@HG1	THR_75@OG1	2.6415	161.0424
PE_1795@O33	LYS_6@HZ2	LYS_6@NZ	2.766	156.5992
PS_1783@O33	ASN_103@HD22	ASN_103@ND2	2.8157	154.011
PE_1795@O33	LYS_6@HZ1	LYS_6@NZ	2.7721	156.4394
PE_1795@O33	LYS_6@HZ3	LYS_6@NZ	2.7639	151.4917
PE_1792@O33	LYS_96@HZ1	LYS_96@NZ	2.7464	158.8401
PS_1783@O33	LYS_102@H	LYS_102@N	2.7913	143.6542
PE_1867@O33	LYS_80@HZ3	LYS_80@NZ	2.7429	156.7533
PE_1828@O12	GLN_99@HE21	GLN_99@NE2	2.7877	157.2343

PE_1852@O12	LYS_10@HZ2	LYS_10@NZ	2.7624	157.0248
PS_1834@O36	LYS_80@HZ3	LYS_80@NZ	2.7546	154.3223
PE_145@O22	LYS_12@HZ2	LYS_12@NZ	2.7716	155.7669
PE_1888@O33	THR_72@HG1	THR_72@OG1	2.6377	164.3975
PE_1828@O22	LYS_97@HZ3	LYS_97@NZ	2.772	154.1763
PC_1858@O34	LYS_102@HZ3	LYS_102@NZ	2.7529	158.052
PE_1828@O22	LYS_97@HZ2	LYS_97@NZ	2.7662	155.9631
PS_1840@O35	LYS_32@HZ1	LYS_32@NZ	2.7703	159.6163
PE_1879@O33	LYS_58@HZ3	LYS_58@NZ	2.7878	155.5272
PE_1828@O33	LYS_97@HZ2	LYS_97@NZ	2.7616	157.7075
PE_1852@O12	LYS_10@HZ1	LYS_10@NZ	2.772	156.9451
PE_1852@O12	LYS_10@HZ3	LYS_10@NZ	2.765	157.3292
PS_1834@O35	LYS_6@HZ3	LYS_6@NZ	2.7775	154.8217
PS_1840@O35	LYS_32@HZ2	LYS_32@NZ	2.777	160.6039
PC_1780@O33	THR_59@HG1	THR_59@OG1	2.7094	157.5654

Table 7.9. Intermolecular Hydrogen bond analysis of membrane bound E46K α-Syn complex during the MD simulation of 100 ns with E46K α-Syn as acceptor and membrane bilayer as donor

#Acceptor	DonorH	Donor	Average Distance (Å)	Average Angle (°)
ASP_115@OD2	PE_1864@HN1B	PE_1864@N31	2.8132	153.824
ASP_115@OD1	PE_1864@HN1B	PE_1864@N31	2.8203	153.6761
GLU_104@OE2	PS_1783@HN1A	PS_1783@N31	2.8146	160.4355
GLU_83@OE2	PE_1894@HN1B	PE_1894@N31	2.7756	158.6446
GLY_101@O	PS_1783@HN1B	PS_1783@N31	2.836	152.8782
GLU_83@OE2	PE_1894@HN1A	PE_1894@N31	2.7739	157.6254
GLU_126@OE1	PS_1837@HN1A	PS_1837@N31	2.7991	156.6697
GLU_104@OE2	PS_1783@HN1B	PS_1783@N31	2.807	160.7232
GLU_104@OE1	PS_1783@HN1A	PS_1783@N31	2.8044	157.2086
GLU_114@OE2	PS_1909@HN1C	PS_1909@N31	2.7969	154.661
GLU_110@OE2	PE_1870@HN1A	PE_1870@N31	2.7769	158.7382
LYS_102@O	PS_1783@HN1A	PS_1783@N31	2.8261	151.9255
GLU_123@OE1	PS_1777@HN1B	PS_1777@N31	2.7745	156.77
ASP_115@OD2	PE_1864@HN1C	PE_1864@N31	2.8176	153.312
GLU_126@OE1	PS_1837@HN1C	PS_1837@N31	2.7954	155.9372
LYS_102@O	PS_1783@HN1B	PS_1783@N31	2.8324	150.5035
GLU_126@OE1	PS_1837@HN1B	PS_1837@N31	2.798	155.6074
GLU_83@OE2	PE_1894@HN1C	PE_1894@N31	2.7796	158.5548
GLY_101@O	PS_1783@HN1C	PS_1783@N31	2.8428	152.719
GLU_104@OE2	PS_1783@HN1C	PS_1783@N31	2.8146	160.3568
ASP_115@OD1	PE_1864@HN1C	PE_1864@N31	2.8245	152.616
THR_72@O	PE_1888@HN1B	PE_1888@N31	2.8172	150.7713
PRO_117@O	PS_1831@HN1A	PS_1831@N31	2.8197	153.8924
GLU_61@OE2	PS_1960@HN1C	PS_1960@N31	2.8067	156.7008
GLU_83@OE1	PE_1894@HN1B	PE_1894@N31	2.7726	157.4065
GLU_123@OE1	PS_1777@HN1C	PS_1777@N31	2.79	155.3859
LYS_102@O	PS_1783@HN1C	PS_1783@N31	2.8327	150.3292
GLU_123@OE2	PE_1846@HN1A	PE_1846@N31	2.7779	156.8129
GLU_114@OE2	PS_1909@HN1B	PS_1909@N31	2.806	154.5776
ASN_103@OD1	PS_1783@HN1B	PS_1783@N31	2.8059	155.5404
GLY_101@O	PS_1783@HN1A	PS_1783@N31	2.8458	151.7024
GLU_104@OE1	PS_1783@HN1C	PS_1783@N31	2.8024	154.3062
THR_92@O	PE_1792@HN1A	PE_1792@N31	2.7874	154.3196
PRO_117@O	PS_1831@HN1B	PS_1831@N31	2.8042	153.1343
THR_75@OG1	PE_1888@HN1B	PE_1888@N31	2.8618	151.9151
GLU_110@OE1	PE_1870@HN1A	PE_1870@N31	2.7824	158.3525
SER_129@OG	PE_1846@HN1C	PE_1846@N31	2.8504	153.1644
THR_72@O	PE_1888@HN1C	PE_1888@N31	2.8281	152.8017
THR_92@O	PE_1792@HN1C	PE_1792@N31	2.8063	150.7184
ASN_103@OD1	PS_1783@HN1C	PS_1783@N31	2.8214	153.287

THR_72@O	PE_1888@HN1A	PE_1888@N31	2.8223	152.4164
GLU_104@OE1	PE_1807@HN1A	PE_1807@N31	2.8069	157.5212
ASP_115@OD1	PE_1864@HN1A	PE_1864@N31	2.8185	153.3574
GLU_110@OE2	PS_1921@HN1A	PS_1921@N31	2.8106	153.0152
GLU_61@OE1	PS_1960@HN1C	PS_1960@N31	2.8132	152.6429
GLU_126@OE1	PE_1786@HN1A	PE_1786@N31	2.7908	153.4693
THR_75@OG1	PE_1888@HN1C	PE_1888@N31	2.8611	150.7007
GLU_126@OE2	PS_1837@HN1A	PS_1837@N31	2.8118	156.62
GLU_110@OE2	PS_1921@HN1B	PS_1921@N31	2.8237	153.7168
GLU_114@OE2	PS_1909@HN1A	PS_1909@N31	2.8134	154.9274

Table 7.10. *Intermolecular Hydrogen bond analysis of membrane bound G51D α-Syn complex during the MD simulation of 100 ns with membrane bilayer as acceptor and G51D α-Syn as donor*

#Acceptor	DonorH	Donor	Average Distance (Å)	Average Angle (º)
PE_1837@O12	LYS_96@H	LYS_96@N	2.8302	161.0856
PE_1810@O12	ASP_98@H	ASP_98@N	2.8088	152.4767
PS_1846@O12	GLU_105@H	GLU_105@N	2.8296	159.9029
PE_1822@O34	THR_59@HG1	THR_59@OG1	2.6283	163.3145
PC_1870@O34	THR_81@HG1	THR_81@OG1	2.6152	165.1441
PE_1807@O22	TYR_136@HH	TYR_136@OH	2.7122	160.7876
PE_1945@O33	SER_87@HG	SER_87@OG	2.6231	165.7489
PS_1813@O34	GLN_62@HE22	GLN_62@NE2	2.8083	164.0007
PS_1786@O34	SER_42@HG	SER_42@OG	2.6089	166.1177
PE_1777@O33	SER_129@H	SER_129@N	2.8296	161.6175
PC_1858@O34	TYR_125@HH	TYR_125@OH	2.6575	162.8583
PS_1801@O33	VAL_118@H	VAL_118@N	2.871	155.1381
PE_1789@O22	GLN_134@HE21	GLN_134@NE2	2.8054	159.3192
PE_1831@O34	LYS_45@H	LYS_45@N	2.8261	162.3659
PE_1810@O33	LYS_96@HZ3	LYS_96@NZ	2.7651	159.2098
PS_1798@O35	SER_87@HG	SER_87@OG	2.5781	165.9615
PS_1783@O33	LYS_97@HZ3	LYS_97@NZ	2.7701	159.1031
PE_1810@O33	LYS_96@HZ2	LYS_96@NZ	2.7644	159.1184
PS_1783@O33	LYS_97@HZ1	LYS_97@NZ	2.7659	158.4333
PC_1816@O33	ASN_103@HD22	ASN_103@ND2	2.7672	155.6695
PS_1783@O33	LYS_97@HZ2	LYS_97@NZ	2.7658	158.6156
PS_1786@O22	LYS_34@HZ3	LYS_34@NZ	2.764	156.7313
PE_1777@O33	SER_129@HG	SER_129@OG	2.6272	166.1821
PS_1798@O36	SER_87@HG	SER_87@OG	2.6141	164.4111
PS_1888@O12	LYS_6@HZ3	LYS_6@NZ	2.7607	154.2575
PE_1810@O33	LYS_96@HZ1	LYS_96@NZ	2.76	158.8177
PE_157@O33	LYS_12@HZ2	LYS_12@NZ	2.7608	158.5139
PS_1786@O22	LYS_34@HZ2	LYS_34@NZ	2.761	157.1819
PC_1795@O34	LYS_80@HZ1	LYS_80@NZ	2.7402	158.4886
PE_1831@O31	LYS_45@H	LYS_45@N	2.885	155.3023

Table 7.11. *Intermolecular Hydrogen bond analysis of membrane bound G51D α-Syn complex during the MD simulation of 100 ns with G51D α-Syn as acceptor and membrane bilayer as donor*

#Acceptor	DonorH	Donor	Average Distance (Å)	Average Angle (º)
ASN_122@O	PE_1771@HN1B	PE_1771@N31	2.8177	151.5611
ASP_115@O	PS_1801@HN1A	PS_1801@N31	2.7907	152.5773
ASN_122@O	PE_1771@HN1A	PE_1771@N31	2.8208	152.1251
ASP_121@OD2	PE_1828@HN1A	PE_1828@N31	2.8146	153.3572
ASP_115@OD1	PE_1903@HN1C	PE_1903@N31	2.8223	158.3186

ASP_121@OD1	PE_1828@HN1A	PE_1828@N31	2.8265	152.0237
ASP_115@OD1	PE_1903@HN1B	PE_1903@N31	2.7977	159.1983
ASN_122@O	PE_1771@HN1C	PE_1771@N31	2.8155	150.9103
ASP_119@OD2	PE_1828@HN1C	PE_1828@N31	2.7923	152.4765
GLU_83@OE2	PS_1888@HN1B	PS_1888@N31	2.7925	157.3388
TYR_125@O	PE_1771@HN1A	PE_1771@N31	2.8168	153.8816
GLU_131@OE1	PE_1777@HN1B	PE_1777@N31	2.777	155.9664
GLU_83@OE2	PS_1888@HN1C	PS_1888@N31	2.7983	157.3388
GLU_83@OE2	PS_1888@HN1A	PS_1888@N31	2.7859	157.7822
ASP_115@O	PS_1801@HN1C	PS_1801@N31	2.7834	151.3124
ASP_121@OD2	PE_1828@HN1B	PE_1828@N31	2.8061	153.8923
ASP_121@OD2	PE_1828@HN1C	PE_1828@N31	2.8189	152.8969
GLU_104@OE2	PS_1846@HN1B	PS_1846@N31	2.7968	156.1168
GLU_131@OE2	PE_1777@HN1C	PE_1777@N31	2.7922	155.9389
ASP_121@OD1	PE_1828@HN1C	PE_1828@N31	2.8207	152.4892
GLU_131@OE1	PE_1777@HN1A	PE_1777@N31	2.7892	154.0785
GLU_104@OE1	PS_1846@HN1A	PS_1846@N31	2.7963	153.271
GLU_123@O	PE_1771@HN1A	PE_1771@N31	2.799	150.2585
GLU_104@OE2	PS_1846@HN1C	PS_1846@N31	2.789	156.8068
ASP_115@OD2	PE_1876@HN1B	PE_1876@N31	2.7669	157.8742
ASP_119@OD2	PE_1828@HN1A	PE_1828@N31	2.8015	153.1086
TYR_125@O	PE_1771@HN1C	PE_1771@N31	2.8129	153.4791
GLU_123@O	PE_1771@HN1C	PE_1771@N31	2.7973	149.9892
GLN_62@OE1	PS_1780@HN1C	PS_1780@N31	2.8113	150.3026
GLU_131@OE2	PE_1777@HN1A	PE_1777@N31	2.7948	155.8717
GLU_123@O	PE_1771@HN1B	PE_1771@N31	2.8099	149.6316
PRO_117@HD2	PS_1801@H1B	PS_1801@C31	2.9175	147.703
ASN_122@OD1	PE_1771@HN1A	PE_1771@N31	2.8308	152.0158
GLU_131@OE1	PE_1777@HN1C	PE_1777@N31	2.7712	157.3412
ASP_115@OD2	PE_1876@HN1C	PE_1876@N31	2.7774	158.3738
ASP_121@OD1	PE_1828@HN1B	PE_1828@N31	2.8282	151.3963
ASP_119@OD2	PE_1828@HN1B	PE_1828@N31	2.8049	153.9473
ASN_122@OD1	PE_1771@HN1B	PE_1771@N31	2.8276	151.3718
ASP_98@OD2	PE_1810@HN1B	PE_1810@N31	2.8032	156.8524
GLU_110@OE1	PE_1903@HN1B	PE_1903@N31	2.7682	155.7243
GLU_131@OE2	PE_1777@HN1B	PE_1777@N31	2.7902	154.3054
ASP_115@OD2	PE_1876@HN1A	PE_1876@N31	2.7787	157.6518
LYS_97@HE3	PS_1783@HR	PS_1783@C1	2.8794	146.1004
ASP_115@O	PS_1801@HN1B	PS_1801@N31	2.7809	148.5854
ASP_115@OD2	PE_1903@HN1C	PE_1903@N31	2.8132	151.8678
ASN_122@OD1	PE_1828@HN1B	PE_1828@N31	2.7845	156.824
THR_92@O	PS_1783@HN1C	PS_1783@N31	2.8141	153.6729
ASP_98@OD2	PE_1810@HN1C	PE_1810@N31	2.7762	157.4988
GLU_104@OE2	PS_1846@HN1A	PS_1846@N31	2.7884	155.1372
ASP_115@OD1	PE_1903@HN1A	PE_1903@N31	2.8045	159.6987

Table 7.12. *Intermolecular Hydrogen bond analysis of membrane bound H50Q α-Syn complex during the MD simulation of 100 ns with membrane bilayer as acceptor and H50Q α-Syn as donor*

#Acceptor	DonorH	Donor	Average Distance (Å)	Average Angle (º)
PE_1840@O33	ASN_103@HD21	ASN_103@ND2	2.791	161.9901
PS_1906@O12	TYR_133@HH	TYR_133@OH	2.7078	164.605
PS_1834@O12	LYS_97@HZ1	LYS_97@NZ	2.7689	156.2836
PC_1771@O34	TYR_136@HH	TYR_136@OH	2.6715	165.891
PE_1801@O33	ASN_103@HD22	ASN_103@ND2	2.8139	156.9886
PS_1834@O12	LYS_97@HZ2	LYS_97@NZ	2.7684	156.5851
PE_1864@O34	GLY_84@H	GLY_84@N	2.7853	152.6327
PS_1813@O12	SER_42@HG	SER_42@OG	2.6771	162.9919
PE_157@O12	LYS_12@HZ3	LYS_12@NZ	2.7638	155.7744
PE_157@O12	LYS_12@HZ2	LYS_12@NZ	2.7672	154.9476

PE_1801@O31	ASN_103@HD22	ASN_103@ND2	2.8626	158.7529
PE_157@O12	LYS_12@HZ1	LYS_12@NZ	2.7606	155.421
PS_1834@O34	GLN_99@HE22	GLN_99@NE2	2.8225	157.6425
PS_1822@O22	GLN_62@HE22	GLN_62@NE2	2.8196	159.4291
PC_1843@O12	GLU_137@H	GLU_137@N	2.8528	155.3495
PS_1834@O12	LYS_97@HZ3	LYS_97@NZ	2.7568	155.8525
PC_1846@O12	LYS_43@HZ1	LYS_43@NZ	2.7724	159.111
PE_1828@O12	LEU_100@H	LEU_100@N	2.8434	150.0612
PC_1846@O12	LYS_32@HZ1	LYS_32@NZ	2.7623	157.4717
PE_1867@O34	LYS_80@HZ3	LYS_80@NZ	2.7224	161.976
PE_1867@O34	LYS_80@HZ2	LYS_80@NZ	2.7262	161.9643
PS_1804@O34	GLN_62@HE21	GLN_62@NE2	2.7863	161.8837
PC_1795@O31	TYR_39@HH	TYR_39@OH	2.7811	157.1206
PS_1834@O33	LYS_97@HZ3	LYS_97@NZ	2.7793	159.128
PE_1885@O34	LYS_32@HZ1	LYS_32@NZ	2.767	156.6901
PE_1852@O22	GLY_41@H	GLY_41@N	2.831	160.4823
PC_1879@O12	GLU_105@H	GLU_105@N	2.8775	161.3321
PC_1789@O34	SER_87@HG	SER_87@OG	2.5961	163.6342
PS_1834@O33	LYS_97@HZ1	LYS_97@NZ	2.7742	156.8103
PC_1879@O34	LYS_102@HZ2	LYS_102@NZ	2.7857	158.1371
PS_1777@O22	SER_87@HG	SER_87@OG	2.6901	159.6593
PE_1885@O34	LYS_32@HZ3	LYS_32@NZ	2.7618	158.4462
PS_1813@O22	SER_42@HG	SER_42@OG	2.6937	161.929
PC_1879@O34	LYS_102@HZ1	LYS_102@NZ	2.7744	157.8284
PE_1867@O12	LYS_80@HZ1	LYS_80@NZ	2.7632	148.996
PE_1882@O33	LYS_45@HZ3	LYS_45@NZ	2.7604	159.7457
PE_1864@O22	LYS_80@HZ2	LYS_80@NZ	2.8081	159.2691
PE_1882@O33	LYS_45@HZ2	LYS_45@NZ	2.7496	158.4444
PE_148@O33	MET_1@H3	MET_1@N	2.7826	155.1882
PC_1879@O12	ASN_103@H	ASN_103@N	2.8628	161.1925
PC_1879@O34	LYS_102@HZ3	LYS_102@NZ	2.7847	156.2264
PS_1813@O35	THR_54@HG1	THR_54@OG1	2.6835	161.5549
PE_148@O33	MET_1@H2	MET_1@N	2.7879	154.5242
PS_1834@O36	LYS_102@HZ1	LYS_102@NZ	2.762	159.6393
PE_1885@O34	LYS_32@HZ2	LYS_32@NZ	2.7456	158.9208
PE_1837@O33	LYS_80@HZ2	LYS_80@NZ	2.7538	157.0332
PE_148@O33	MET_1@H1	MET_1@N	2.7812	153.3499
PS_1774@O35	LYS_96@HZ3	LYS_96@NZ	2.7645	156.8409
PE_1837@O33	LYS_80@HZ1	LYS_80@NZ	2.769	155.8664
PE_1882@O33	LYS_45@HZ1	LYS_45@NZ	2.7513	158.6128

Table 7.13. *Intermolecular Hydrogen bond analysis of membrane bound H50Q α-Syn complex during the MD simulation of 100 ns with H50Q α-Syn as acceptor and membrane bilayer as donor*

#Acceptor	DonorH	Donor	Average Distance (Å)	Average Angle (⁰)
GLU_83@OE2	PE_1837@HN1A	PE_1837@N31	2.8092	153.6177
GLU_83@OE1	PE_1837@HN1A	PE_1837@N31	2.8017	152.7259
GLU_123@OE1	PS_1783@HN1A	PS_1783@N31	2.7637	154.9902
GLU_105@OE2	PE_1927@HN1B	PE_1927@N31	2.7871	155.6174
GLU_123@OE2	PS_1783@HN1A	PS_1783@N31	2.7677	156.263
GLU_137@OE1	PE_1870@HN1B	PE_1870@N31	2.7755	154.037
GLU_139@OE1	PS_1762@HN1C	PS_1762@N31	2.7989	156.1104
GLU_123@OE2	PS_1783@HN1C	PS_1783@N31	2.7629	154.3127
GLU_123@OE1	PS_1783@HN1B	PS_1783@N31	2.7774	155.1766
GLU_131@OE2	PE_1798@HN1B	PE_1798@N31	2.7962	148.9901
GLU_83@OE2	PE_1837@HN1C	PE_1837@N31	2.8155	153.9559
GLU_123@OE1	PS_1783@HN1C	PS_1783@N31	2.767	154.4948
GLU_83@OE1	PE_1837@HN1C	PE_1837@N31	2.8002	151.527
GLU_83@OE2	PE_1837@HN1B	PE_1837@N31	2.8025	153.2979
THR_59@OG1	PE_1885@HN1C	PE_1885@N31	2.8488	156.9565

GLU_83@OE1	PE_1837@HN1B	PE_1837@N31	2.8014	153.7476
MET_116@O	PS_1876@HN1A	PS_1876@N31	2.8031	154.3473
ALA_91@O	PS_1777@HN1C	PS_1777@N31	2.8146	155.5726
ASP_115@OD1	PE_1900@HN1C	PE_1900@N31	2.7793	156.8852
MET_116@O	PS_1876@HN1C	PS_1876@N31	2.7998	155.2167
GLU_104@O	PE_1840@HN1C	PE_1840@N31	2.7963	154.3487
GLU_114@OE1	PS_1876@HN1A	PS_1876@N31	2.7962	157.2221
GLU_131@OE2	PE_1798@HN1A	PE_1798@N31	2.8039	154.317
GLU_126@OE1	PS_1825@HN1A	PS_1825@N31	2.7896	156.8424
GLU_137@OE1	PE_1870@HN1C	PE_1870@N31	2.7699	150.6934
GLU_126@OE2	PS_1825@HN1A	PS_1825@N31	2.7996	158.4199
GLU_131@OE1	PE_1798@HN1B	PE_1798@N31	2.8171	153.636
GLU_123@O	PS_1783@HN1B	PS_1783@N31	2.8137	151.7512
GLU_139@OE1	PE_2527@HN1B	PE_2527@N31	2.7715	154.7841
MET_116@O	PS_1876@HN1B	PS_1876@N31	2.8038	154.7204
GLU_105@OE2	PE_1927@HN1C	PE_1927@N31	2.8016	155.3906
ALA_91@O	PS_1777@HN1B	PS_1777@N31	2.8123	155.4048
GLU_105@OE1	PE_1927@HN1C	PE_1927@N31	2.7928	153.3071
GLU_105@OE1	PE_1831@HN1B	PE_1831@N31	2.7764	157.3737
THR_59@OG1	PE_1885@HN1A	PE_1885@N31	2.8534	157.7092
LYS_58@O	PS_1804@HN1C	PS_1804@N31	2.8371	155.0053
GLU_139@OE1	PE_2527@HN1A	PE_2527@N31	2.7759	158.0767
GLU_104@O	PE_1840@HN1B	PE_1840@N31	2.8019	152.3384
GLU_114@OE2	PS_1876@HN1B	PS_1876@N31	2.7974	155.577
GLU_137@OE1	PE_1870@HN1A	PE_1870@N31	2.7841	152.0391
GLU_130@OE2	PE_1861@HN1A	PE_1861@N31	2.7856	155.1682
GLU_104@O	PE_1840@HN1A	PE_1840@N31	2.7996	153.9999
GLU_105@OE2	PE_1831@HN1B	PE_1831@N31	2.769	158.9511
GLU_123@O	PS_1783@HN1C	PS_1783@N31	2.8081	151.3602
GLU_114@OE1	PS_1876@HN1C	PS_1876@N31	2.7964	155.6093
GLU_114@OE1	PS_1876@HN1B	PS_1876@N31	2.8054	157.6024
GLN_62@O	PS_1822@HN1A	PS_1822@N31	2.8181	155.4765
ALA_91@O	PS_1777@HN1A	PS_1777@N31	2.8117	155.405
GLN_62@O	PS_1822@HN1B	PS_1822@N31	2.8257	158.7263
THR_59@OG1	PE_1885@HN1B	PE_1885@N31	2.8366	158.0528

7.4.7. Conformational snapshots of α-Synuclein mutants:

Throughout the MD simulation of the α-Syn mutants were found to undergo rapid conformational changes. The snapshots of the α-Syn mutants at different time period were generated using UCSF Chimera v.1.13.1 (**Figures 7.8-7.13**) [306]. For the α-Syn mutants, the trajectory snapshots were obtained every 20 ns for further analysis. The NAC region is responsible for the aggregation propensity of α-Syn protein. From the snapshots, it was observed that the NAC region of A30P α-Syn mutant among all other mutants showed to have higher degree of extending out of the membrane. The nature and extent of aggregation are shown to be influenced by membrane curvature and the shape or orientation of the protein. The N-terminal region is believed to be the anchor of the α-Syn protein. In our study, the N-terminal region of H50Q mutant α-Syn is showed to have highest insertion into the membrane surface that suggest the stability of the protein as compared to other α-Syn mutants. In comparison to the WT α-Syn as discussed in section **4.4.8**, the α-Syn protein was observed to have broken down in the non-amyloidogenic region and found to elevate above the surface similar to A30P

α-Syn mutant. However, the degree of insertion allows the protein structure to maintain its stability during the MD simulation.

(A)

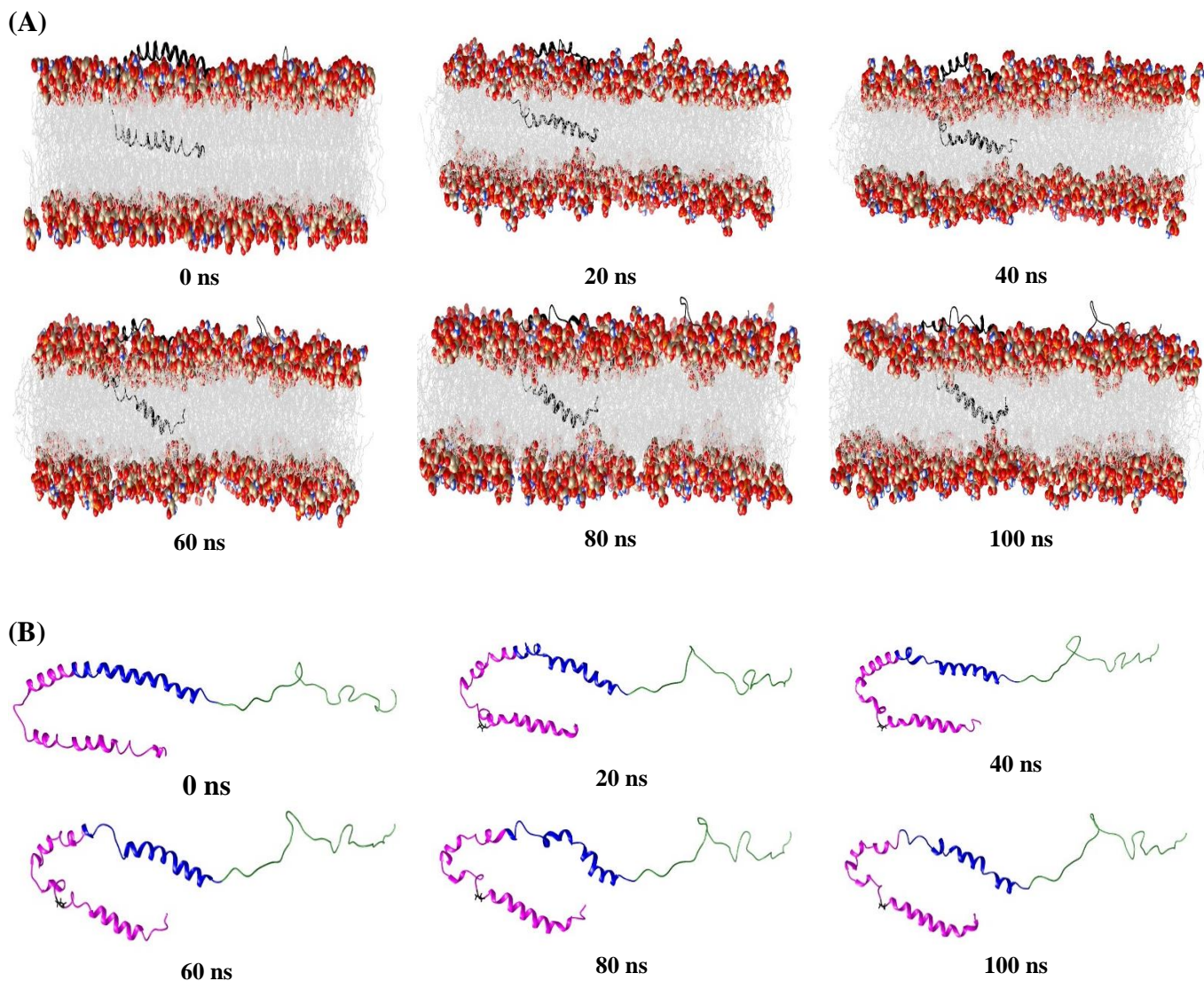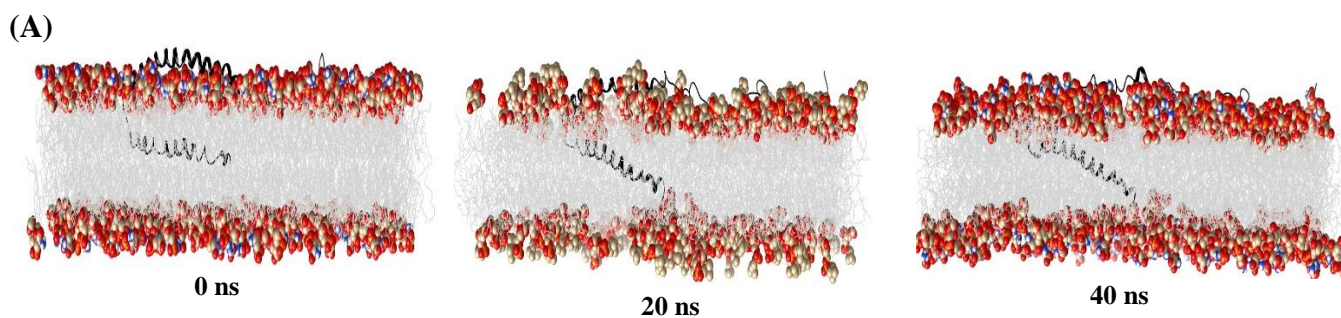|		
0 ns	**20 ns**	**40 ns**
60 ns	**80 ns**	**100 ns**

(B)

0 ns	**20 ns**	**40 ns**
60 ns	**80 ns**	**100 ns**

Figure 7.8. *Conformational snapshots of (A) membrane bound A30P α-Syn and (B) membrane hidden as a function of simulation time*

(A)
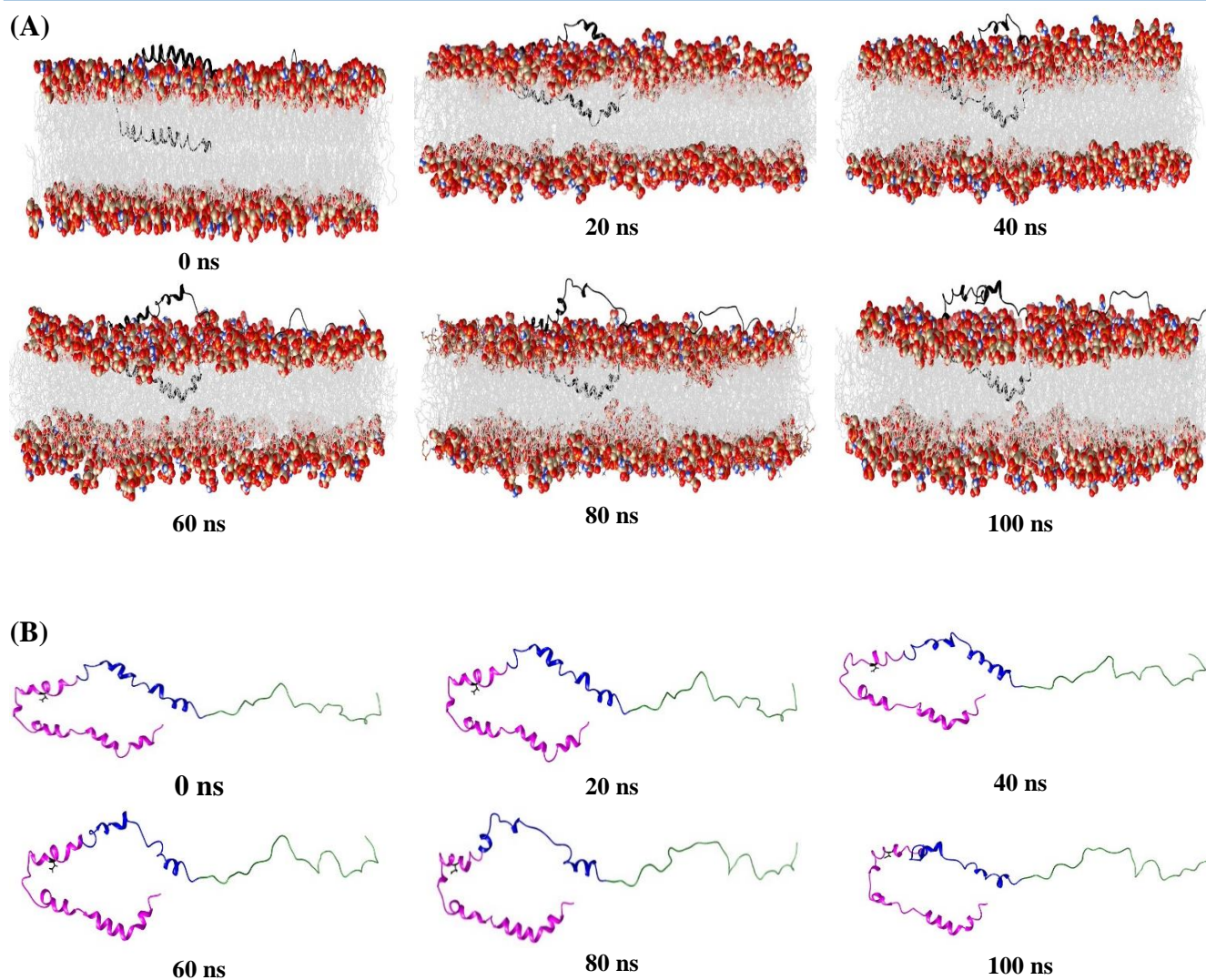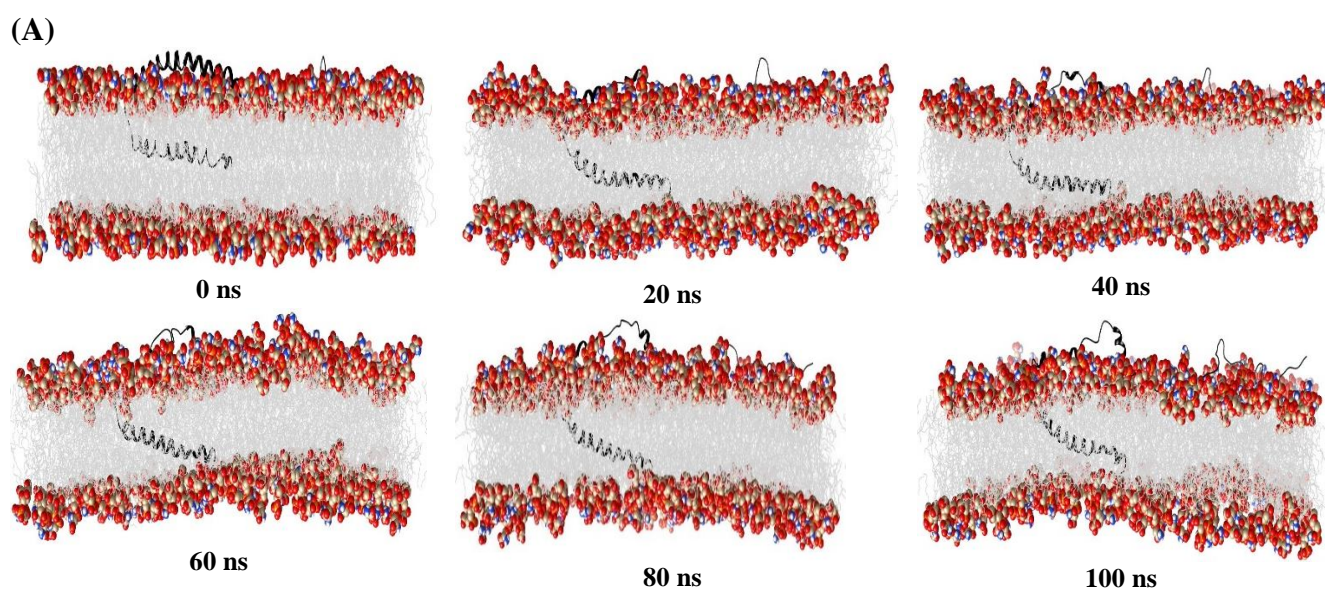

0 ns	**20 ns**	**40 ns**

(B)
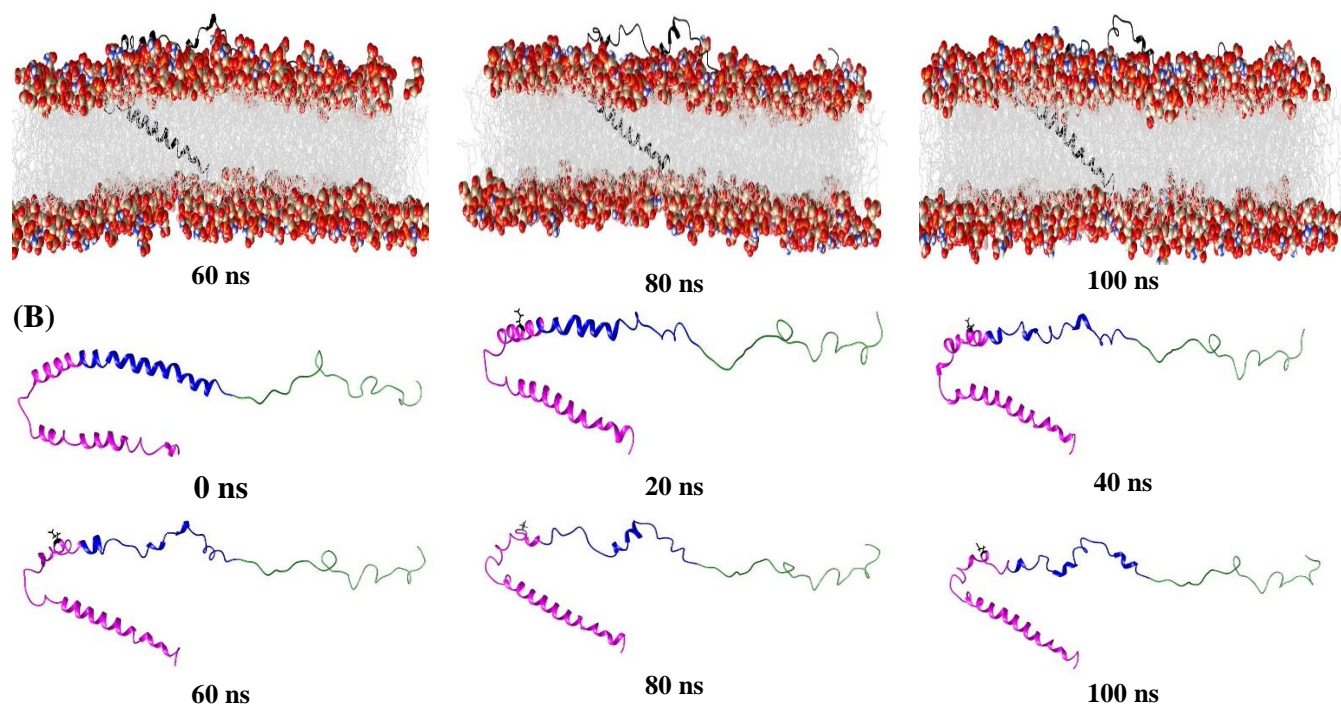
Figure 7.9. *Conformational snapshots of (A) membrane bound A53E α-Syn and (B) membrane hidden as a function of simulation time*

(A)

(B)

60 ns   80 ns   100 ns
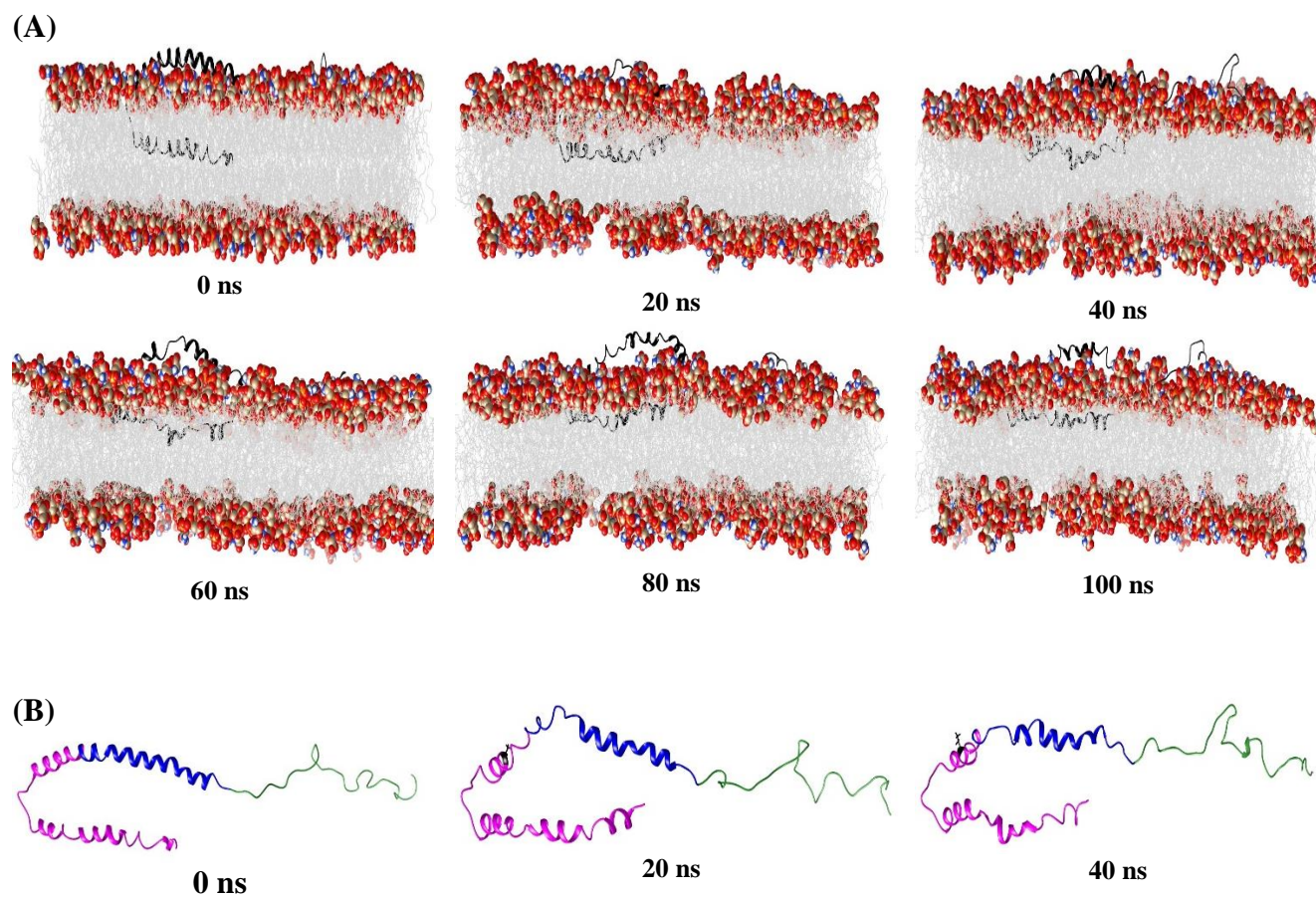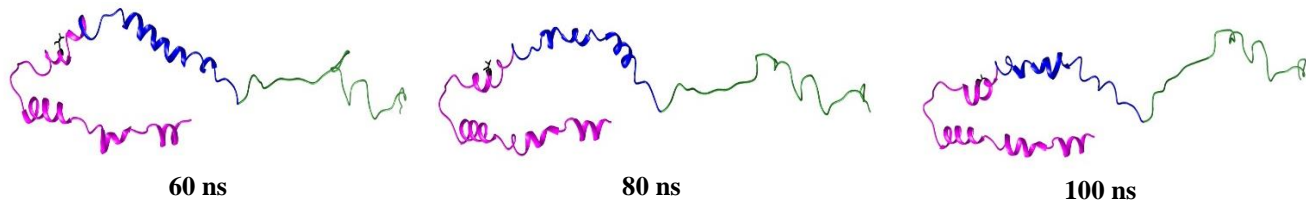
Figure 7.10. *Conformational snapshots of (A) membrane bound A53T α-Syn and (B) membrane hidden as a function of simulation time*

(A)

0 ns   20 ns   40 ns

60 ns   80 ns   100 ns

(B)

0 ns   20 ns   40 ns

60 ns   80 ns   100 ns
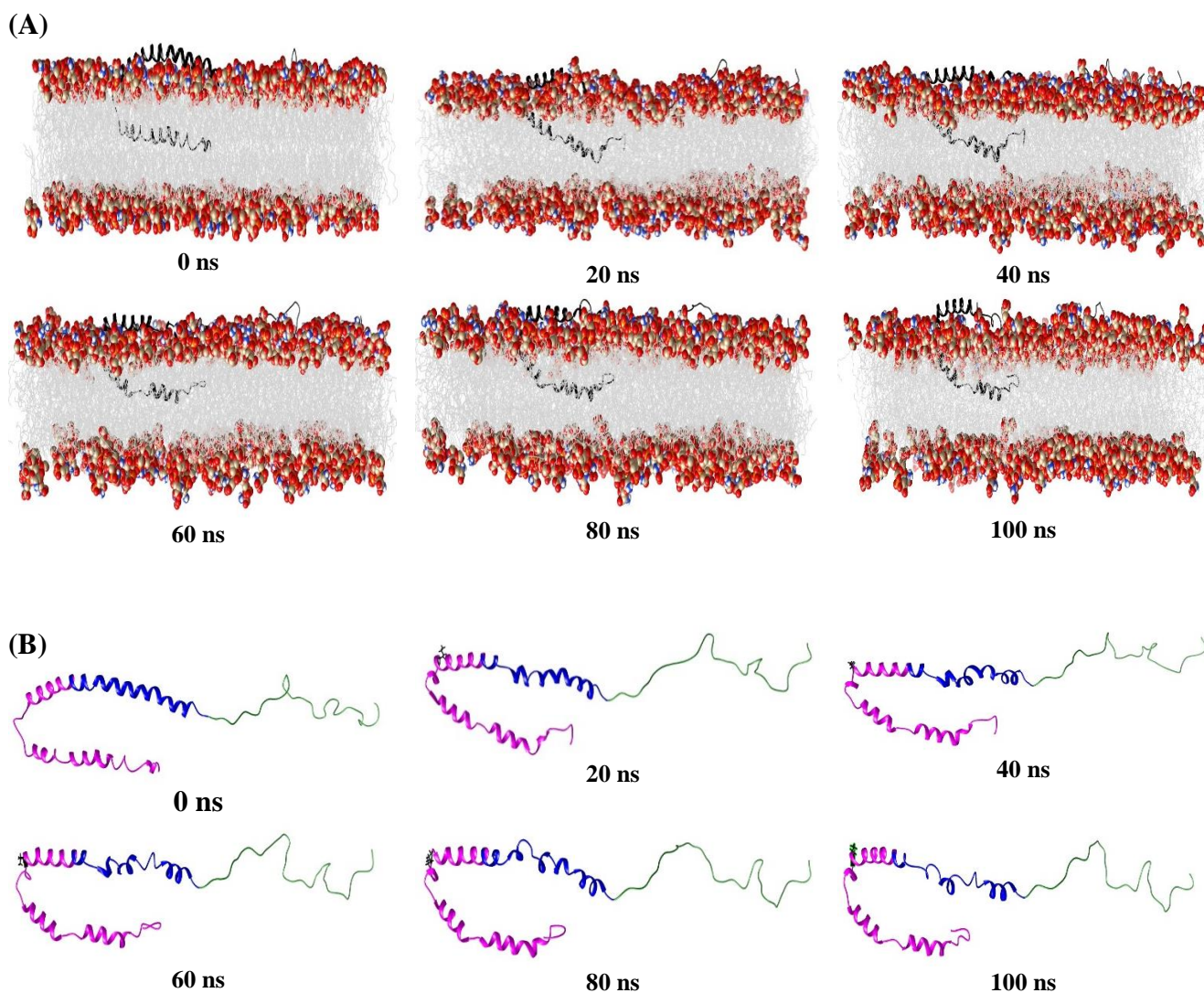
Figure 7.11. *Conformational snapshots of (A) membrane bound E46K α-Syn and (B) membrane hidden as a function of simulation time*

(A)

0 ns   20 ns   40 ns

60 ns   80 ns   100 ns

(B)

0 ns   20 ns   40 ns

60 ns   80 ns   100 ns

Figure 7.12. Conformational snapshots of (A) membrane bound G51D α-Syn and (B) membrane hidden as a function of simulation time

(A)

0 ns   20 ns   40 ns

60 ns   80 ns   100 ns

(B)

0 ns   20 ns   40 ns

60 ns   80 ns   100 ns
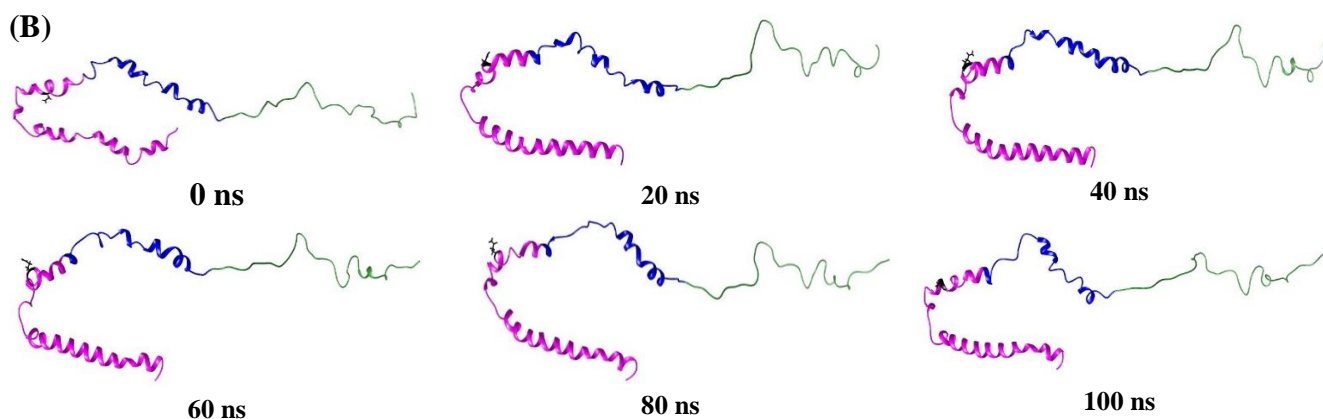
Figure 7.13. *Conformational snapshots of (A) membrane bound H50Q α-Syn and (B) membrane hidden as a function of simulation time*

7.4.8. Secondary structural analysis:

The DSSP program incorporated into the Kabsch and Sander algorithm [295] was used to determine the secondary structure of the α-Syn mutants as shown in **Figure 7.14**. **Figure 7.14(A-F)** show the secondary structure variation of each residue as a function of frame numbers for the α-Syn mutant complexes. The secondary structure of IDPs exhibits β-sheets, which are indicative of aggregation and have also demonstrated that the existence of secondary structures may trigger the α-Syn aggregation process [483, 484]. The percentage probability score of α-Syn mutants were determined as observed in **Figure 7.15(A-F)**. In **Table 7.14**, the secondary structure analysis of all the mutants also showed that there is an increase in the presence of anti-parallel β-sheet structure of the A30P and A53E α-Syn mutants as compared to the α-Syn protein as calculated in **Table 4.1**. The percentage of α-helix was observed to be the highest in case of H50Q α-Syn mutant (41.4%) followed by A30P (38.6%), E46K (36.4%), A53T (22.1%), G51D (21.4%). However, the helical content in A53E α-Syn mutant (17.9%) was calculated to be lower than WT α-Syn (18.9%) as seen in **Table 4.1**. Thus, it can also be remarked that the H50Q α-Syn mutant protein has the most stable conformation and therefore influence the aggregational propensity of the α-Syn structure.
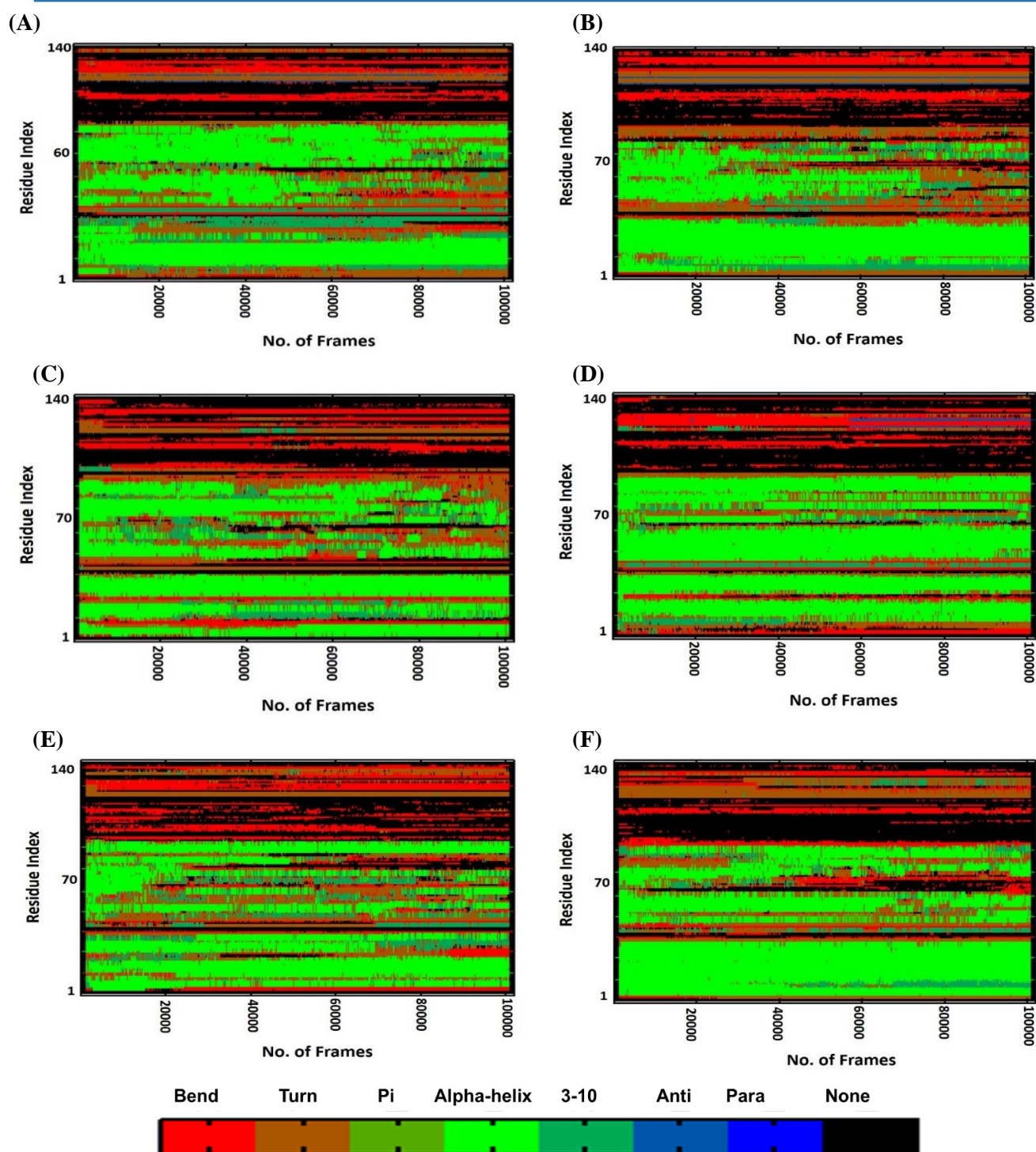
Figure 7.14. DSSP plot of (A) A30P, (B) A53E, (C) A53T, (D) E46K, (E) G51D and (F) H50Q α-Syn mutants using Kabsch and sander algorithm
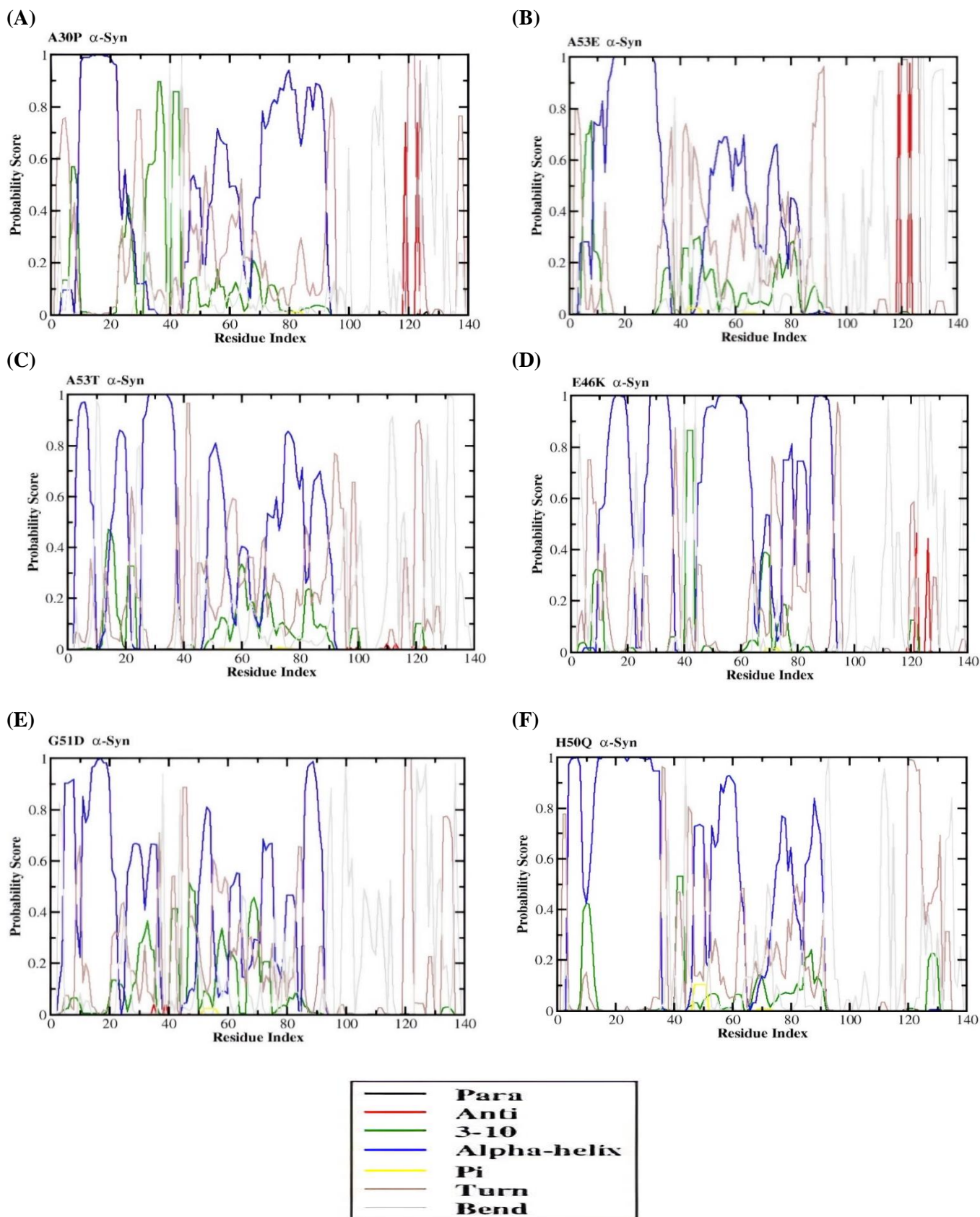
(A)

(B)

(C)

(D)

(E)

(F)

Figure 7.15. Percentage secondary probability score of (A) A30P, (B) A53E, (C) A53T, (D) E46K, (E) G51D and (F) H50Q α-Syn mutants and lipid membrane

Table 7.14. Secondary structural content of all the α-Syn mutants during MD simulation

Mutant α-Syn	α-helix %	β-sheet %	turn %	Pi-helix %	3-10 helix %	Coil %
A30P	38.6	2.1	18.6	0	0	40.7
A53E	17.9	2.1	27.1	0	4.3	48.6
A53T	22.1	0	20	0	8.6	49.3
E46K	36.4	0	8.6	0	0	55
G51D	21.4	0	25.7	0	0	52.9
H50Q	41.4	0	17.1	0	0	41.4

7.4.9. Distance analysis:

The center of mass distance between N-terminal and C-terminal regions of α-Syn mutants were measured for the membrane bound mutant α-Syn systems. The separation between the N-terminal and the C-terminal was evaluated over the course of the simulation by analyzing their individual trajectory files. We have measured the distance between the N-terminal and C-terminal domains of all the α-Syn mutants as shown in **Figure 7.16.** From the plot, it is evident that over time, the distance between the N-terminal and the C-terminal of E46K α-Syn gradually decreasing while the overall structure of the A53T α-Syn showed consistent shorter distance between N-C terminals. The higher distance between N-C terminals of α-Syn mutants suggests more stability as seen in A53T α-Syn mutant.
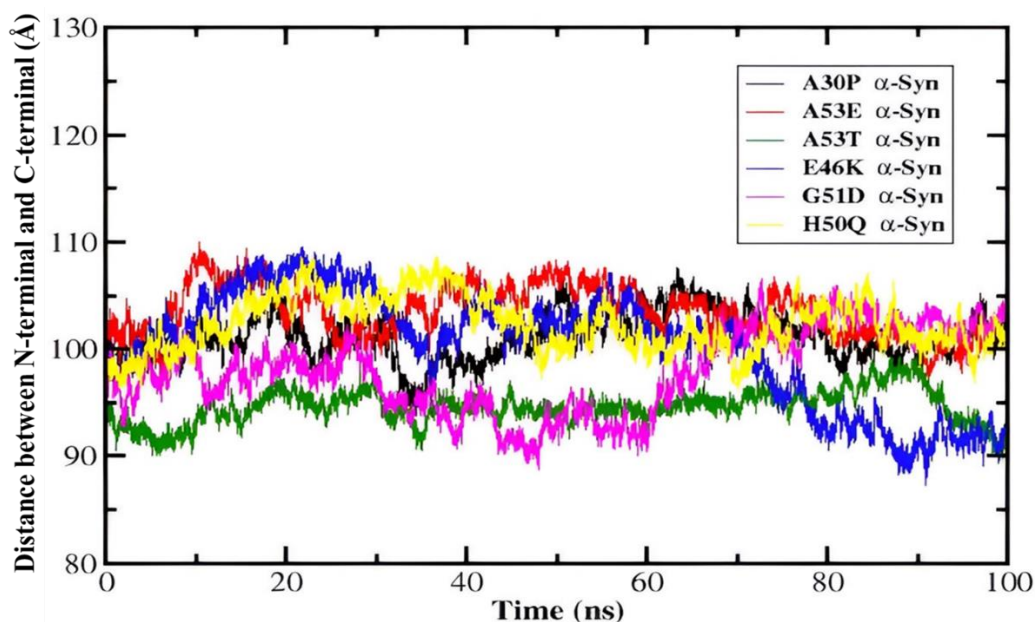

Figure 7.16. Distance analysis between N-terminal and C-terminal of membrane bound α-Syn mutants as a function of simulation time

7.5. Conclusion:

This study provides an insightful comparative analysis of the conformational dynamics of α-Syn mutants (A30P, A53E, A53T, E46K, G51D and H50Q) using all-atom MD simulation. The trajectories obtained from the MD analysis were analyzed to determine the overall stability of the α-Syn mutants. From the RMSD profiles of all the mutants, E46K α-Syn mutant was found to be most stable but A53E α-Syn showed higher instability among others. The nature and extent of aggregation are shown to be influenced by membrane curvature and the shape or orientation of the protein. A30P α-Syn mutant slightly destabilizes and alters the protein's helical structure around the site of the mutation. The distance analysis plots suggested that higher distance between N-terminal and C-terminal indicated more stability as seen in A53T α-Syn compared to other mutant α-Syn proteins. In our study we have observed membrane curvature in H50Q α-Syn mutant as compared to other mutant in α-Syn. The secondary structural content analysis was found to retain higher structural conformity in the case of H50Q α-Syn, while percentage of A53E α-Syn showed α-helical content close to WT α-Syn. Therefore, further research is needed to address these mutational effects and pinpoint the mechanisms that cause disruption in PD.